**NOVA**FCSH

FACULDADE DE CIÊNCIAS SOCIAIS E HUMANAS
UNIVERSIDADE NOVA DE LISBOA

# Assessing the geometry and tuning properties of historical timbilas through non-destructive reverse engineering techniques

Eduardo Fernandes Lopes de Oliveira

**Master's Dissertation in Musical Arts**

**July, 2020**

Dissertation presented to meet the requirements for obtaining a Master's degree in Musical Arts, conducted under scientific advice of Vincent Georges Mickael Debut

Dissertação apresentada para cumprimento dos requisitos necessários à obtenção do grau de Mestre em Artes Musicais, realizada sob a orientação científica de Vincent Georges Mickael Debut

*Ao vô Sérgio*

**Assessing the geometry and tuning properties of historical timbilas through non-destructive reverse engineering techniques**

**EDUARDO FERNANDES LOPES DE OLIVEIRA**

**[ABSTRACT]**

Timbilas are xylophones finely manufactured and tuned by the Chopi people from Mozambique. In the context of a research project, we aim at assessing the construction and acoustical features of a set of historical instruments by developing non-destructive characterization techniques based on reverse engineering, with main objectives to assess their original tuning and musical scale. In this thesis, we present the methodology and workflow that have been developed for the study of the collection of historical timbilas of the National Museum of Ethnology of Lisbon, which is the world's largest collection of the Mozambican instrument. In a first stage, contactless geometrical measurements were performed on a nine-bar timbila by using 3D scanning Technology, resulting in a detailed geometrical description of the instrument bars. In a second stage, the 3D collected geometrical data was used as input to Finite Element computations in order to calculate the modal frequencies and mode shapes of each bar of the instrument. Results stemming from our modal computations were compared with modal data obtained from vibrational measurements, proving the efficiency of the proposed approach. Final stage was using the data as input for developing a sound synthesis model for recreating the sound of the timbila bars.

Keywords: Reverse engineering, modal analysis, 3D scanning technology, African xylophones.

# [RESUMO]

Timbilas são xilofones cuidadosamente construídos e afinados pelos Chopes, povo de Moçambique que cultiva uma das mais importantes tradições musicais do sul da África. No contexto de um projeto interdisciplinar de investigação, objetivamos avaliar as características geométricas e acústicas de alguns exemplares históricos, desenvolvendo técnicas não-destrutivas de caracterização baseadas num processo de engenharia reversa, com o principal objetivo de avaliar a afinação e a escala musical de um conjunto de instrumentos. A metodologia desenvolvida consiste no levantamento preciso da geometria das barras a partir de tecnologia de imagens scanner 3D, resultando numa descrição detalhada de sua morfologia. Num segundo passo, realizamos cálculos modais a partir de um modelo por Elementos Finitos 3D construido a partir dos dados coletados, a fim de calcular as frequências modais e formas vibratórias das principais ressonâncias de cada barra do instrumento. Os resultados dos cálculos modais foram finalmente comparados com os valores de parâmetros modais identificados a partir de medições vibratórias, demonstrando a utilidade e eficácia da metodologia proposta. O estágio final foi a utilização dos dados para criar um modelo de síntese sonora para as barras da timbila.

Palavras-chave: Engenharia reversa, análise modal, Elementos Finitos, scan 3D, xilofones africanos

# Contents

# Chapter 1

# Introduction

Timbilas are rare xylophones finely manufactured and tuned by Chopi people from Mozambique. During a last century strongly affected by political and economical difficulties, the country has progressively lost many aspects of tangible memory of timbila: famous musicians died, practical know-how has been left to industrialized production and the new generation has lost touch with tradition, while it has been mainly based on hereditary knowledge transmission (Tracey, A., 2011).

As a rare testimony of historical timbila, the National Museum of Ethnology of Lisbon houses the world's most representative collection, which mainly dates back to the late 1940s. These instruments offer to musicologists an opportunity to revisit and challenge research on Chopi xylophones, reviving interest in timbila music and in the construction of instruments following traditional techniques. However, before attempting any systematic study of instruments of the museum collection, preliminary work is needed, and this is the aim of this dissertation: to develop a characterization technique in order to assess their acoustical and musical features, following the principles of preservation and conservation of museums.

We therefore propose a non-destructive approach based on 3D scanning technology and reverse engineering techniques, and develop a systematic methodology in order to provide insights into the tuning of the bars and the reference pitch of the instruments. The proposed approach provides a precise description of the bars geometry and results in a full 3D virtual model that can be extensively used for analysis of the bar vibrational properties,

thus informing the instrument tuning features and for developing computer simulations, thus providing a basis for developing virtual instruments of traditional timbila.

## 1.1   Context of the work

This dissertation was carried out in the context of a FCT funded research project called *Music research and new technologies towards the restitution of the timbila collection of the National Museum of Ethnology*, coordinated by Professor João Soeiro Carvalho and Professor Vincent Debut, from the Instituto de Etnomusicologia – Centro de Estudos em Música e Dança. The project is intended to explore a shared methodology, bridging Ethnomusicology and Music Acoustics in an effort to implement an inspiring safeguarding framework for the restitution of Chopi timbila's tradition to Mozambique. The importance of safeguarding timbila was acknowledged in 2005 by UNESCO, which proclaimed it a Masterpiece of the Oral and Intangible Heritage of Humanity.

> The *Intangible Cultural Heritage* means the practices, representations, expressions, knowledge, skills – as well as the instruments, objects, artifacts and cultural spaces associated therewith – that communities, groups and, in some cases, individuals recognize as part of their cultural heritage. This intangible cultural heritage, transmitted from generation to generation, is constantly recreated by communities and groups in response to their environment, their interaction with nature and their history, and provides them with a sense of identity and continuity, thus promoting respect for cultural diversity and human creativity (UNESCO, 2003, pg. 5).

With this proclamation, one of UNESCO intentions is to raise awareness, especially among the younger generations, of the importance of the intangible cultural heritage and of its safeguarding, and encourage local communities to protect and sustain these forms of cultural expressions. The UNESCO document defines safeguarding as measures aimed at ensuring the viability of the intangible cultural heritage, including the identification, documentation, research, preservation, protection, promotion, enhancement, transmission, particularly through formal and non-formal education, as well as the revitalization of the various aspects of such heritage. It proposes an action plan defining safeguard strategies, with goals established according to the reality and the needs identified in each country.

In the case of Mozambican timbila, one of the aspects defined as priority by the

government is the teaching of timbilas manufacturing (Agencia Lusa, 2020). For that matter, the present project can be a valuable tool, as its final stage consists in sharing the knowledge obtained with musicians and researchers in Mozambique, in partnership with the School for Arts and Communication of Eduardo Mondlane's University and from the Archives for Cultural Heritage (Arpac) from Mozambique's Ministry of Culture. This meets another of the goals pointed by Unesco, which is to stimulate international cooperation and assistance, in a global effort to preserve cultural manifestations menaced by social and political instabilities.

Portugal and Mozambique have a strong historical bond, full of cultural affinities which are important to preserve and strengthen. That makes Portugal a natural agent on the restitution of the Timbila culture, especially considering that the largest collection of historic instruments is in its territory. The study of this collection offers an unique opportunity to scientifically revisit our knowledge of the instrument, contributing to the literature about timbila's construction and establishing scientific knowledge about important acoustical features that make it such an unique instrument.

Furthermore, another output of this project will be the recreation of these historical timbilas on the digital realm, by developing a musical production plug-in compatible with the main recording and musical performance softwares. The characterization methodology developed in this dissertation allows us to obtain a solid physicalmethodology for the representation of the functioning of the Timbilas, which can be used as input for sound synthesis by physical modeling.

The development of technologies of this nature contributes in a tangible and lasting way to the conservation of the timbila's cultural heritage. In an age of virtual instruments and digital music production, it is an essential step for preserving this musical manifestation to posterity, helping to keep this tradition alive and accessible so that musicians can incorporate it in the most different musical languages. It makes the timbila universally accessible, along with the symbolic dimension associated with it. That way, this project not only aims at preserving the cultural heritage of the Chopi people, but also makes it available to those who shape music in the present, thus investing in its future relevance.

## 1.2   Timbila and the Chopi people

The Chopi people are one of several ethnic groups in the southern region of Mozambique. The timbila tradition is associated to the Zavala district, in the province of Inhambane, about 350 km from the capital, Maputo (Figure 1.1). The fine manufacturing and tuning of the instruments reflect the artistic and technical knowledge of Chopi communities.
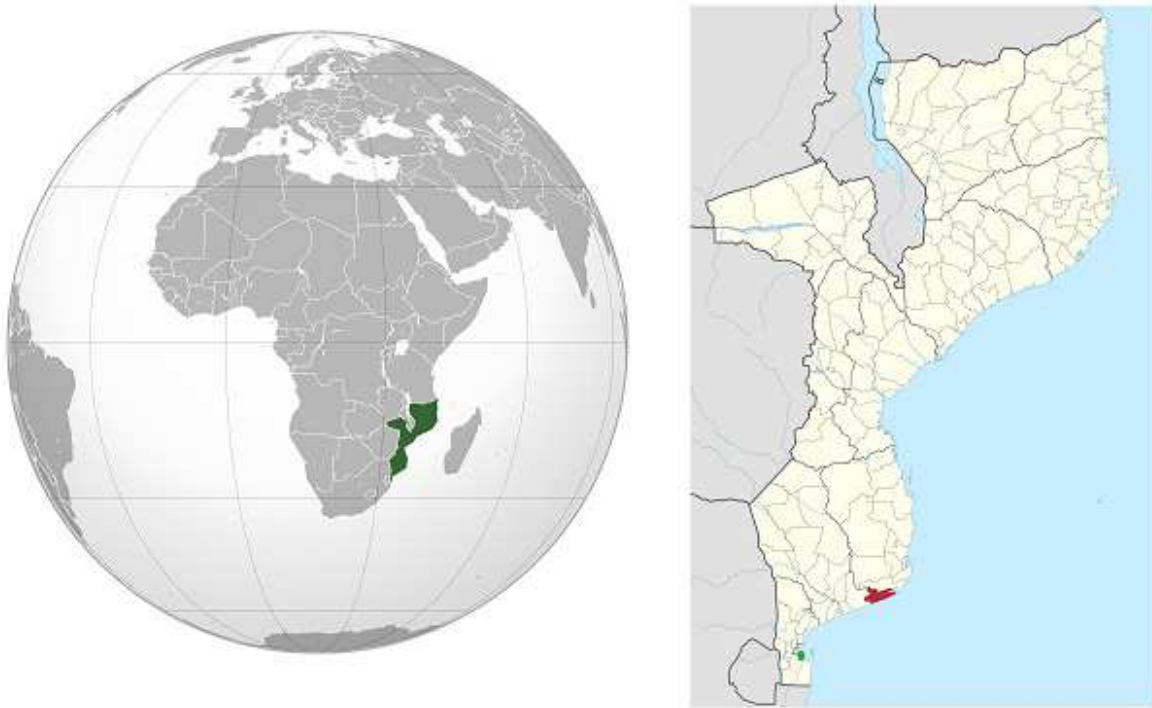


**Figure 1.1:** Left: African map with Mozambique marked in green. Right: Mozambiquean map with the Zavala district marked in red and the capital, Maputo, in green (from Wikipedia).

The oldest written records of timbila Chopi date back to the 16th century, a time when the Portuguese started establishing their presence in this region of Africa as a consequence of the exploration of new commercial routes to the Indies. Since then, the populations there established have been influenced not only by the Portuguese, but also by other African kingdoms and traders of Arab origin, present for centuries in the region (Wane, M., 2010).

It is, therefore, a constantly adapting cultural expression that has survived the most diverse political and socio-economic changes. Reports of expeditions describing the timbila culture through the centuries are also valuable historical documents on the structure of society, as the words sung by the Chopes portray a very straight picture of current social issues. The oldest reports point them singing about kings and tribal leaders. During Portuguese

colonialism, the exploitation imposed by the metropolis was the main theme.

A common aspect observed through the years is the good humor and irony to talk about the daily lives of the communities and to criticize or praise leaders. It constitutes a forum where many issues are discussed, having a social impact to the communities (Wane, M., 2010). The text can be considered a kind of social conscience that interprets public events impartially and distributes sometimes criticism and praise, thus contributing to a certain democratic balance in society (Dias, M., 1966).

Nowadays, the timbila is present at several social events in the Chopi community, such as weddings, birthdays, initiation rites, agricultural rites etc (Wane, M., 2010). Although originated in Zavala, the timbila culture is not restricted to that district, having its representation in several surrounding villages. They all gather once a year in august for the *Msaho* music festival, which takes place in the village of Quissico, in Zavala.

The *Msaho* originated as a local event, having undergone several reformulations over time, and today it promotes social interaction between different populations. Each timbila orchestra represents the place where it comes from, symbolizing the prestige of each locality, in an environment of regional competition. It is the main event to celebrate the timbila culture, gathering not only the population of neighboring towns, but also national and foreign tourists, in an atmosphere of festive celebration.

Timbila music and poetry is usually accompanied by cycles of dance and singing, on very well structured theatrical performance called Ngodo, which consists of 8 to 11 articulated parts, with some variations from orchestra to orchestra. Like the movements of a symphony orchestra, the sections of the timbila performance are composed of different musical and choreographic arrangements, which correspond to different poetic forms (Wane, M., 2010).

For the ethnomusicologist João Soeiro de Carvalho, it is impossible to understand a cultural manifestation such as the timbila from a mere separation of its components. The categorization of music, dance, theater and poetry is defined from a Western epistemological conception, therefore the author suggests its definition as a whole, which he calls "expressive modality".

In the case of Southern African cultures, body motion, sound production and drama are closely

associated in a wholeness-generating behavior. This is an integrated phenomenon, perceived and culturally defined according to criteria which encompass rules of gravity to the awareness of different constituents. These include body movement, sound production, stage settings, text, drama, etc. Emphasis on each of these constituents by the performers themselves, or novelty of perception by the observer, results in different cognitive experiences – and its resulting descriptions – of the performing phenomena (Carvalho, J. S. de, 1999, pg. 149).

Although this dissertation is focused on the musical aspect of the timbila – on the instrument itself, to be more precise – a global understanding of this cultural manifestation is key to study how the instrument evolved over the years, with the ever-changing shaping of the chopi culture. Tuning, scales and manufacturing techniques are all subject to changes caused by the interactions of the society. It constitutes a cyclic relation where the culture shapes the instrument as the instrument shapes the culture.

# Chapter 2

# Historical contextualization

## 2.1  Early ethnomusicological background

"These fortunate people are much given to the pleasures of singing and playing". The words written in 1562 by Father André Fernandes, in a letter addressed from Goa to the Brothers and Fathers of the Society of Jesus in Portugal, prove that the musicality of Chopi people has been alive for long. The Jesuit missives are the oldest records portraying the wonders of timbila music and the existence of the Mozambican xylophones, which he richly described.

> Their instruments are many gourds bound together with cords, and a piece of wood bent like a bow, some large and some small, and to the openings in which they fasten trumpets with the wax of wild-honey to improve the sound, and they have their treble and bass instruments. At night they serenade the king and anyone who has made them a present, and he who makes the most noise is accounted the best musician. Their songs are generally in praise of him to whom they are singing, as 'this is a good man, he gave me this or that, and will give me more' (Theal, G. M. C., 1898, pg. 283).

Over the following centuries, the timbila often appeared in reports of expeditions on southern Africa. Dos Santos (Dos Santos, J., 1609) gives a detailed description of a 18 bar instrument, and evaluates it as "producing a sweet and rhythmical harmony, which can be heard as far as the sound of a good harpsychord". La Caille (de La Caille, N.L., 1763) described it as "tolerably sonorous, and with its twelve notes a great many tunes can be played upon it". Wangemann (Wangemann, D., 1898) wrote about instruments consisted of bars and

gourd resonators played by two men at the same time, adding that "the tones sounded both soft and loud".

In the 20th century, with the increased European presence in Africa, the ethnomusicological reports began to appear in greater number. Junod (Junod, H. A., 1929) presented a very comprehensive article about the timbila, detailing the construction of the instrument and the functioning orchestras with help of illustrations (Figure 2.1). "This interesting instrument has been developed by the T/opi *(sic)* people with such a perfection that we might be justified in considering it as a distinct and genuine production of the T/opi genius. The other bantu tribes surrounding them do not hesitate to call the Vat/opi the 'masters' of the mbila"(Junod, H. A., 1929, pg. 275). In 1934, Percival R. Kirby (Kirby, P. R., 2013) published a very comprehensive encyclopedia on musical instruments from southern Africa, with a chapter dedicated to the timbila, mostly based on Junod work, but adding photographs and transcriptions in score.



"Msaho wa mkoma" at the kraal of Chief Maḍatin, Zandzamela
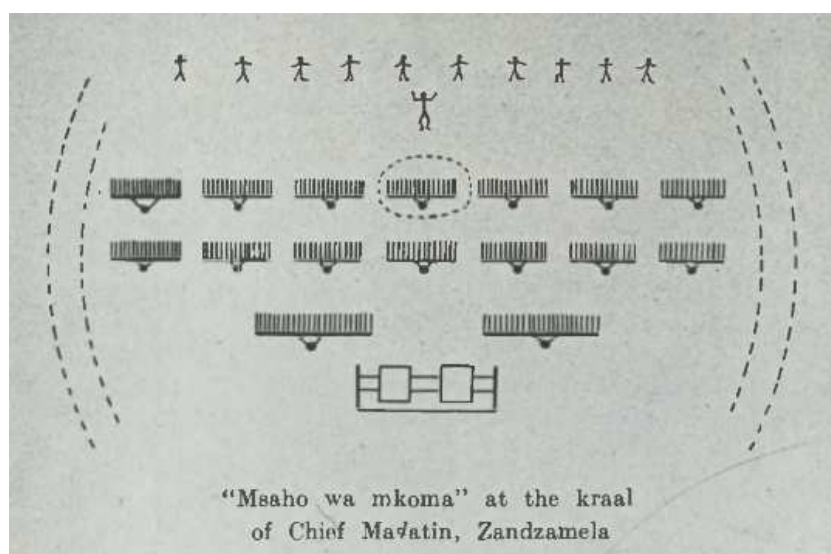
**Figure 2.1:** Illustration of a timbila orchestra (Junod, H. A., 1929, pg. 283).

In 1948, the ethnomusicologist Hugh Tracey (Tracey, H., 1948) set the cornerstone to the literature on the timbila, with the publishing of the book *Chopi Musicians: Their Music, Poetry and Instruments*. Tracey dedicated his life to document the musical culture in Southern Africa, and, up until now, his work has been the reference to most of what has been published about Chopi music and dance. The book discusses the poetry on which the music and dances are based, provides a glossary of musical terms and analyses some of the musical compositions and their structure with illustrations and transcriptions in score.

In a four year expedition, the author established a deep relation with leading Chopi musicians and instrument makers, which results in a very detailed description of the timbila mechanics, methods of manufacture and tuning techniques. The researcher was very well impressed with the skills of players, the knowledge of the makers and the quality of the instruments.

> Timbila of the Chopi are perhaps the most interesting of the musical instruments of the southern Bantu. (...) the Chopi instrument is as good as, if not better than, the majority of its kind on this continent. (...) It is excellently made by skilled craftsmen.(...)The Chopi are well aware of the natural laws controlling the production of sound so far as their type of instrument is concerned. (...) Chopi musicians are by far the most musically developed in southern Africa (Tracey, H., 1948, pg. 118, 122, 141).

Ethnomusicologist Margot Dias also praised the musicality of the Chopes when she wrote about her expeditions to Mozambique on the 60's, which resulted in a series of articles and a book that was published 20 years later. "The artistic ability of Mozambicans is best proved in the musical field itself. In Mozambique, some forms of music stand out above the general level. The most prominent example are the marimbas orchestras, an important element of the chopi culture" (Dias, M., 1966, pg. 14).

## 2.2 Recent years - Colonial wars, independence and globalization

On the second half of the 20th century, Mozambiquean culture was deeply affected by political and social instability. After a violent Portuguese resistance and about a decade of armed struggle against colonialism, the country gained independence and was constituted as a national state in June 1975. However, the warfare was far from over. Once independent, Mozambique was governed by the Front for the Liberation of Mozambique (FRELIMO) - a Marxist-Leninist party constituted by the merging of nationalist pro-Independence movements, supported by the Soviet socialist bloc. Its borders with South Africa, Africa's main capitalist power, placed Mozambique on the African front of the Cold War, involving the country in a civil war, with opponents FRELIMO and the National Resistance of Mozambique (RENAMO), an organization supported by South Africa and the capitalist bloc (Wane, M.,

2010).

The armed conflict that began in 1976 only ended 16 years later, leaving a balance of about 1 million dead, the destruction of the country's infrastructure and leaving great part of the population on poverty, especially in rural areas (Wane, M., 2010). After the reestablishment of peace in 1992, the country has since gone through a reconstruction of its cultural identity. Therefore, recent ethnomusicology has particularly underlined the dynamics of cultural performance as social action (Carvalho, J. S. de, 1999).

In an age of globalization, another central point of ethnomusicological discussion is the influence of Western cultures on the shaping of African culture.

> Attitudes towards native or foreign traditions and performers' perception of the fusion of Western and African elements provide valuable insights into the understanding of culture change. The coexistence of Western and non-Western elements in performance may constitute an analogy to other levels of social phenomena, and thus help to create more general analytical procedures in social studies (Carvalho, J. S. de, 1999, pg. 153).

Ethnographic studies from the past decades increasingly pointed out the influence of a western dominated globalized culture on traditional African manifestations, a reality that also applies to the timbilas. On an article published in 1980, ethnomusicologists Martinho Lutero and Carlos Martins Pereira (Lutero, M. and Pereira, C. M., 1980) revealed the presence of a large number of timbilas tuned in diatonic scales, in order to be used for performances of western compositions.

> It's not just about changing the pitch of an instrument's notes, but about changing the whole musical hearing of a people. Imagine, for example, that suddenly our current pianos changed the relationship of notes to each other. The pianists would have to change their entire technique of playing the instrument. The music that came out would sound quite different from what we are used to today. A series of changes that would turn the current culture around (Lutero, M. and Pereira, C. M., 1980, pg. 586).

This kind of influence is nothing new. Tracey (Tracey, H., 1948) already described timbilas tuned in western scales so the orchestras could perform the portuguese anthem during visits of leaders of the metropolis. In an ever more globalized society, this kind of interference raises the question of the mischaracterization of certain indigenous cultural manifestations due

18

to the unequal contact with western culture (Wane, M., 2010).

This is an important aspect to be considered on a international cooperation on the safeguarding of the timbila as cultural heritage. It is a process that requires a deep relation between foreigner researchers and the locals, taking in account the Chopi relation with music and their perception of it, in opposition to simply applying a western epistemology to the subject, which may cause even more interference to the local culture.

20

# Chapter 3

# Acoustical contextualization

## 3.1 Timbila xylophones

Timbila is a musical instrument of the xylophone family. Xylophones can be defined as wooden percussion idiophones. An idiophone is any musical instrument that creates sound primarily by the object vibrating as a whole. Percussion idiophones produce sound by being struck with a foreign object, like mallets, hammers or sticks. The timbral characteristics of percussion instruments is governed by the radiated vibrations of their modes. The impulsive strike of the mallet excites the eigenmodes which generally do not form a harmonic series of overtones, since the mode frequencies and their ratios depend on the material and shape of the vibrating parts of the instrument (Bork, I. et al., 1999). On bar instruments, the bending transverse vibrations (Figure 3.1) are dominant, and deserve careful attention. However, other modes, including torsional modes, can also be excited (Chaigne, A. and Kergomard, J., 2016).

In the most improved xylophones, the bars are parallel to each other, supported on nodes in the first vibrating mode and arranged in a similar way to a keyboard. Under the bars there are usually resonators that intensify its vibration, and hence the sound of the instrument. The series of bars produce sounds of varying pitch, which is determined by the material, length and thickness of the bars. The tuning is done by excavation process, removing mass from the bar at appropriate points (Henrique, L., 2004). Traditional xylophones are basically tuned in three types of scales: pentatonic, hexatonic and heptatonic (Nketia, 1975). Although the use of equidistant systems is more widespread, systems of unequal intervals are also found
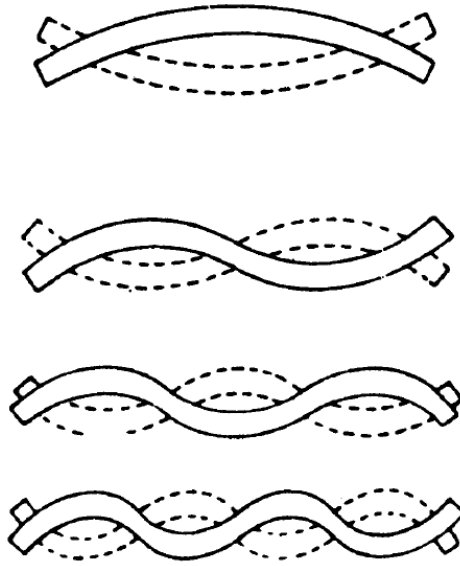
21

**Figure 3.1:** First vertical flexural modes of a bar with constant cross-section with free-free boundary conditions.

(Jones, A. M., 1964).

## 3.2   Construction

Each bar of the instrument is called mbila (Figure 3.4) –  which can be translated as note – timbila being the plural.  The Mbila is made of a wood called *Mwenje (Ptaeroxylon obliquum)*, which comes from a tree in the process of extinction.  Hugh Tracey's writings show that its extinction was already a concern in 1948. "The *Mwenje* tree is only found in one small region of the Zavala district.  The trees grow in a thickly wooded portion of the country and are not very numerous" (Tracey, H., 1948).  In an article published in 1949, the researcher shows astonishment for the wide knowledge of the musical properties of woods by native instrument makers.

> The choice by the Chopi musicians of a certain hard wood, *Ptaeroxylon obliquum*, for the notes of their xylophones, appears not only to be the best for their district but the only reverberating wood of any quality in that area. In addition to knowing the general musical quality of this wood, they had also found that the female of this dioecious species was more resonant than the male, and that the portion of the tree most musically effective was the root.  How did they come by this knowledge?  Empirically or by sheer accident?  They arrived in their present geographical locality early in the 16th century, and it appears unlikely that they had any previous knowledge of this tree, which does not grow in the country of their origin.  (Tracey, H., 1949, pg. 17)

22

The bars are mounted on a wooden frame, in general made of the *Mukusu wood* (Figure 3.3). A hole is made in one of the nodal points of the first vibrating mode of the bars (Figure 3.4), which are suspended by bark strings or thongs of hide straps that hold them together (Figure 3.3). At the bottom of the board are attached a series of gourd resonators of different sizes (Figure 3.3). The resonators are generally made of *Matamba*, the hard peel of a wild fruit. The junction of the resonator with the board is caulked with beeswax (Figure 3.3).

In addition to the hole oriented towards the board opening, each resonator has a side hole (Figure 3.5). This is covered by a very thin membrane, made either of a rodent's diaphragm, an ox's peritoneum or a bat's wing. The membrane is protected by a piece of tube made of certain trees or the neck of gourds (Figure 3.5). The vibration of the air in the gourd forces the membrane to resonate, adding a hum to the sound of the blade. The resonators are tuned in sympathy with each of its respective bar. Finally, the beaters are made of wooden sticks, with a ball of rubber of the *Mbungo tree*. Both the size and the hardness of the drumsticks vary substantially depending on the instrument used. Musicians can even use a stick of different hardness in each hand.

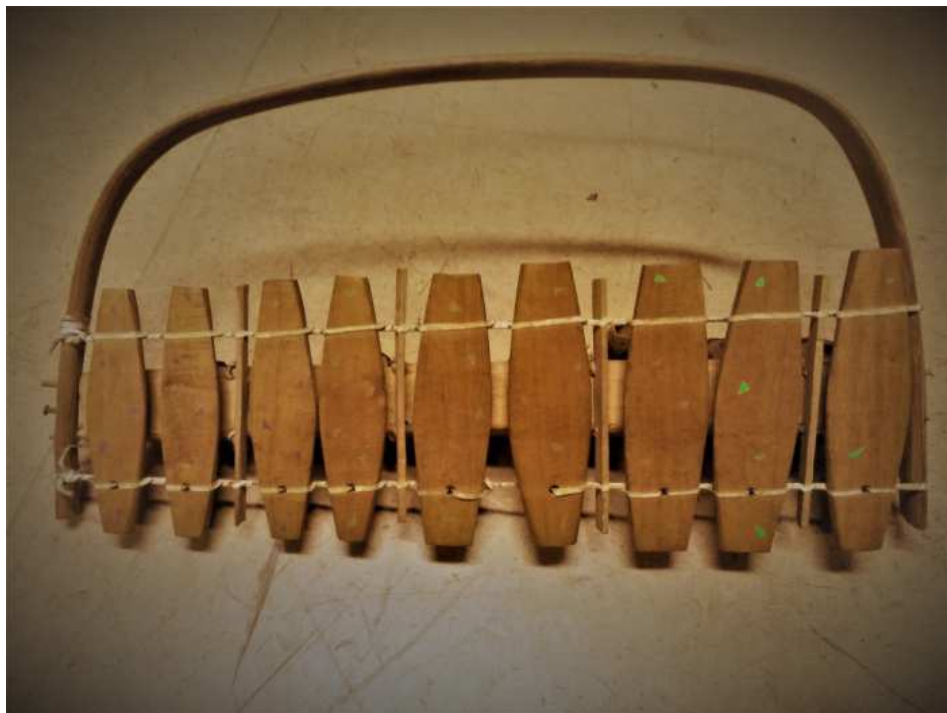

**Figure 3.2:** The laboratory 9-bar timbila investigated in this work.

**Figure 3.3:** (a) Wooden frame; (b) flexible cord holding the bars; (c) resonator, (d) bee wax to affix resonator.
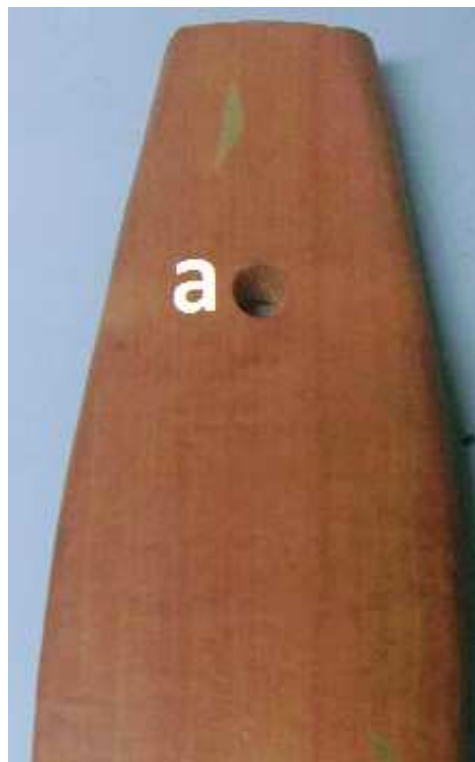


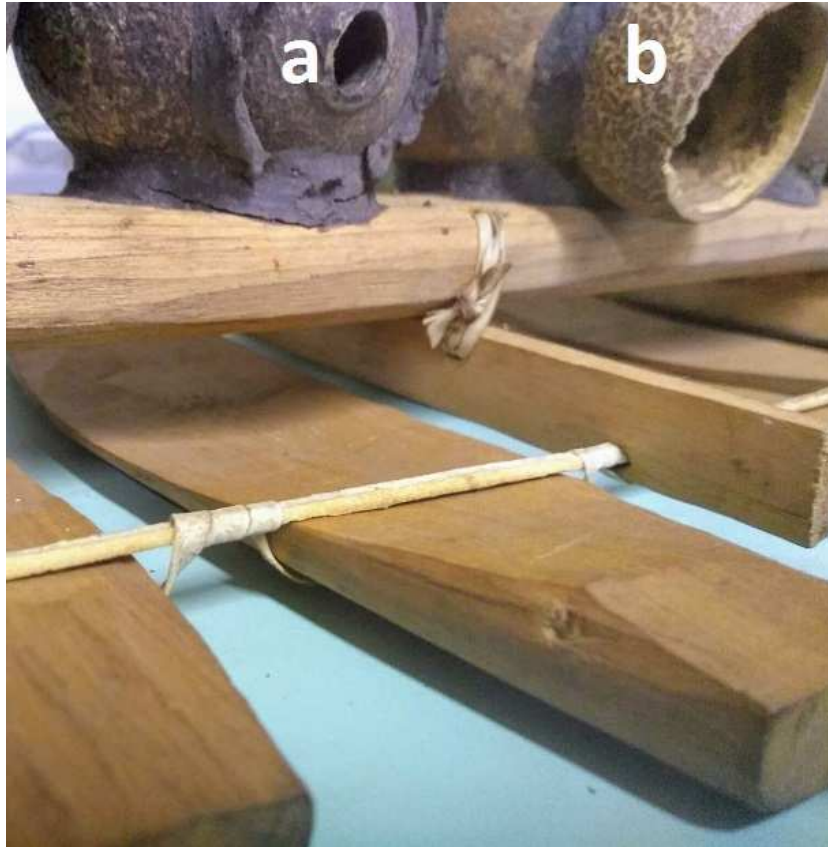**Figure 3.4:** Drilled hole in the bar for fixture.

**Figure 3.5:** (a) Side hole of resonator; (b) protective tube.

## 3.3   Tuning

Timbilas are made to be primarily played in ensembles. The orchestra consist in five kinds of timbilas, covering a range of four octaves, with overlaps between the instruments. Hugh Tracey classified these instruments according to their range, in an analogy with the western orchestras. The high end is covered by the *Cilanzane* or *Malanzane*. With 12 to 16 mbilas, it can be called the treble timbila. The first note of it is called *Hombe*, which is the keynote for the tuning of the instruments. The alto instrument is called *Sange* or *Sanje*. It adds 1 to 3 notes below the *Hombe* and has a total of 14 to 18 bars. It is the instrument played by the leader and also the most numerous on an orchestra. The tenor timbila is called *Dole* or *Mbingwe*, starting 4 or 5 notes below the *Hombe* and with a total of 10 to 14 notes. The bass instrument, *Debiinda*, starts one octave below the *Hombe* and has 10 bars. Finally, *Khulu* or *Gulu*, the double bass, consists in only 3 or 4 notes, starting 2 octaves below the *Hombe*. The distribution of notes can be better understood on Figure 3.6.

In his work, Hugh Tracey investigated several hundred of historical timbilas,

Figure 3.6 table:

| | Number | Name of note and range | Instrument | | | | |
|---|---|---|---|---|---|---|---|
| | | | Cilanzane | Sange | Dole | Debiinda | Gulu |
| Octave″ | 16 | digumi nidimwedo | × | × | | | |
| | 15 | digumi nicanu | × | × | | | |
| | 14 | digumi nimune | × | × | | | |
| | 13 | digumi nimararu | × | × | | | |
| | 12 | digumi nimambidi | × | × | | | |
| | 11 | digumi dimwedo | × | × | | | |
| | 10 | digumi | × | × | | | |
| | 9 | nimune | × | × | | | |
| Octave′ | 8 | Hombe idoko | nimararu | × | × | | | |
| | 7 | nimambidi CILANZANE | × | × | × | | |
| | 6 | nedimwedu | × | × | × | | |
| | 5 | canu | × | × | × | | |
| | 4 | mune | × | × | × | | |
| | 3 | mararu | × | × | × | × | |
| | 2 | mambidi | × | × | × | × | |
| Tonic | 1 | HOMBE | dimwedo | × | × | × | × | |
| | 3 | mararu | | × | × | × | |
| | 2 | mambidi SAŊGE | | × | × | × | |
| | 1 | dimwedo | | × | × | × | |
| | 4 | mune | (×) | × | × | | |
| | 3 | mararu | | × | × | | |
| | 2 | mambidi DEBIINDA | | | × | | |
| ,Octave, | 1 | (Hombe) dimwedo | | | × | | |
| | 4 | mune | | | | | × |
| | 3 | mararu GULU | | | | | × |
| | 2 | mambidi | | | | | × |
| ,,Octave,, | 1 | (Hombe) dimwedo | | | | | × |

**Figure 3.6:** Range and distribution of notes in a Chopi orchestra (Tracey, 1948, p. 125).

analyzing their tuning and musical scale systematically. His work was based on frequency measurements obtained using a set of tuning forks, seeking aid of native musicians for choosing the right tuning-fork to correspond to each note. The tuning of the *Hombe* was found to vary slightly according to the location, ranging from 252 Hz to 276 Hz (see Figure 3.7).

| | Zavala | Chisiko | Mavila | Banguza | Zandamela |
|---|---|---|---|---|---|
| Octave | 504 | 512 | 520 | 520 | 552 |
| | 456 | 472 | 464 | 472 | 496 |
| | 408 | 424 | 424 | 432 | 448 |
| | 368 | 384 | 384 | 388 | 408 |
| | 336 | 348 | 352 | 356 | 368 |
| | 304 | 316 | 320 | 316 | 336 |
| | 276 | 288 | 284 | 288 | 308 |
| Hombe | 252 | 256 | 260 | 260 | 276 |

**Figure 3.7:** Reference tuning in Hertz used in orchestras of four distinct districts (Tracey, H., 1948, pg. 120).

Tracey describes a meeting he held with musicians and timbilamakers from different districts, with whom he had an in-depth discussion about their tuning techniques. After the meeting, the chief timbilamaker from Zandamela – the one with the most deviant tuning in relation to the other districts– decided to change the tuning of his distric to Zavala's.

It was most enlightening to hear them argue as to which was the most correct pitch for the

tone centre, *Hombe*. Katini maintained that, as the Paramount Chief's musician, his was the one and only correct pitch, his was the 'king's note', vouchsafed to him by his father, grandfather, and ancestors who had been hereditary leaders and composers of the king's music for generations (Tracey, H., 1948, pg. 124).

This shows the very hereditary nature of the knowledge transmission. "Like many other country crafts, the manufacture of musical instruments is often found in families, the art being handed down from father to son" (Tracey, H., 1948, pg. 129). Despite the controversy on the central note, they seemed to agree on the scale sought to tune the rest of the bars, a kind of tempered heptatonic scale. "They all agreed that each in his own way was attempting to achieve the same kind of scale, an even scale of seven intervals, all alike" (Tracey, H., 1948, pg. 124). Tracey further describes the tuning process:

> Having tuned the *Hombe*, the maker now tunes his scale up to the octave, every note in turn up the scale. He attempts to give each interval exactly the same value, and this accounts for the Chopi disregard for the true fourth and fifth which in other parts of Africa are often the first intervals to be tuned. Once the initial scale is complete up to the octave of *Hombe*, called by some *Hombe idoko*, the little *Hombe*, the musician runs over his notes and makes certain they are as even as he can get them. Then, from there onwards, the tuning of the remaining notes is done in octaves from this central scale. As a rule their octaves are true and exact (Tracey, H., 1948, pg. 138).

The work by Tracey still remains a major reference on timbilas, considering the amount of studied instruments and his close relationships with makers and musicians, and it can be interesting to review and revisit some of his main findings. For the five studied timbilas, Figure 3.8 shows the intervals between successive notes along the musical scale. As seen, they are actually nearly constant, close to the value of 171.42 cents [1], which is the theoretical musical interval corresponding to a heptatonic musical scale. Moreover, looking at the dispersion of the intervals between instruments, one notices that the fourth and the fifth have a more consistent tuning than the other intervals, thus justifying the comments by Tracey that "some of them still cling to the inclusion of perfect fourth and perfect fifth in the scale" (Tracey, H., 1948, pg. 128).

Rather than using the measured value for the *Hombe*, which can be more or less accurate due to errors in tuning or during measurements, one can attempt to estimate the

---

[1] The cent is the micro-interval equal to one hundredth of a tempered semi-tone: 1 cent = $2^{1/12} = 1.0595$.
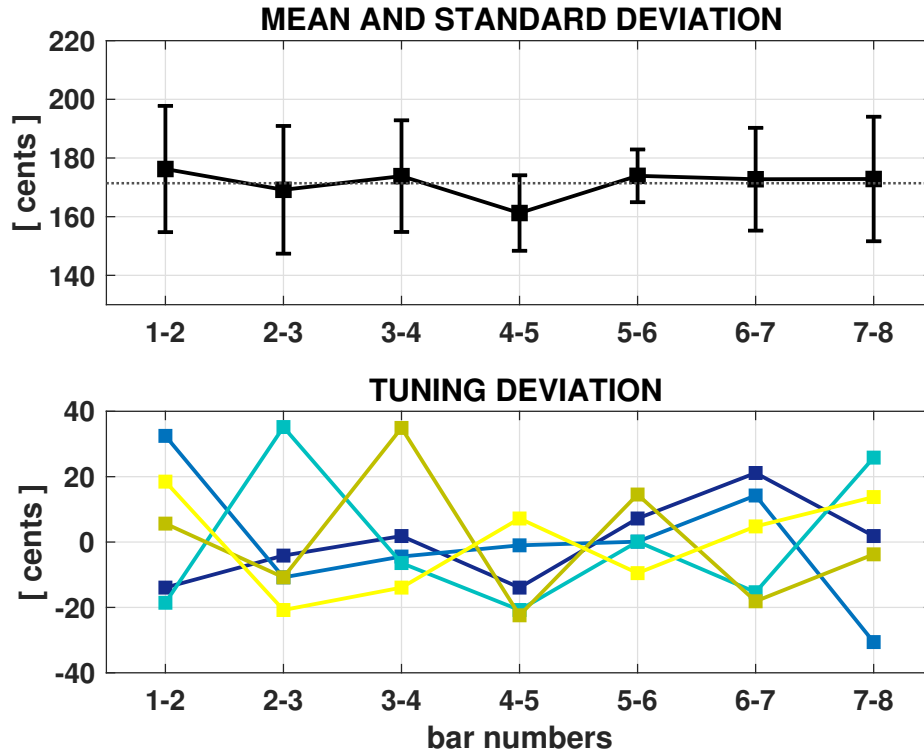
**Figure 3.8:** Original timbilas measured by Tracey (Tracey, H., 1948). Top: means and errors of intervals between instruments in relation to an heptatonic scale based on the *Hombe* frequency of the instruments. Bottom: tuning deviation between successive bars for each timbila.

reference frequency of the musical scale by devising a similar strategy as proposed by Debut et al. (Debut, V. et al., 2016a) for historical carrillons, but here assuming a perfectly-tuned equi-heptatonic musical scale. Instead of looking at the fundamental frequency of a single bar, this approach estimates the reference pitch by accounting for all the bars comprising the instrument, thus balancing possible bars that could be mistuned in the scale.

Table 3.1 lists the computed reference pitches for the five instruments, which are close to the values presented by Tracey, as one could anticipate. As can be seen, the difference in frequency for the *Hombe* falls within the frequency resolution of Tracey, which was $\pm 2$ Hz, and thus gives confidence in his analysis.

Figure 3.9 then presents the tuning deviations of each bar for the five instruments regarding the computed values. Notably, one observes that tuning errors are in the range of $\pm 20$ cents about the expected values and that fifths are particularly well-tuned, except for the Zavala instrument, thus highlighting a specific attention by makers in relation to these intervals. This justifies Tracey's comment about the inclusion of perfect fourth and perfect

fifths in some orchestras, and that the Zavala orchestra actually favors the perfect fourth instead of the perfect fifth, according to musicians.

Other interesting aspect is to look at the overall dispersion in tuning of each instrument regarding the equi-heptatonic musical scale based on the *Hombe* tone, which is a mean of comparing the tuning quality of the instruments. As seen in Figure 3.9, the dispersion in tuning deviation for the five instruments is in the range of [10-15] cents, thus providing some quantitative information about the tuning abilities of makers. Finally, notice that these errors are small and close to the tunability range of human hearing.

**Table 3.1:** Measured $f$ and computed $f^\star$ frequencies for the *Hombe* tone of instruments studied by Tracey (Tracey, H., 1948).

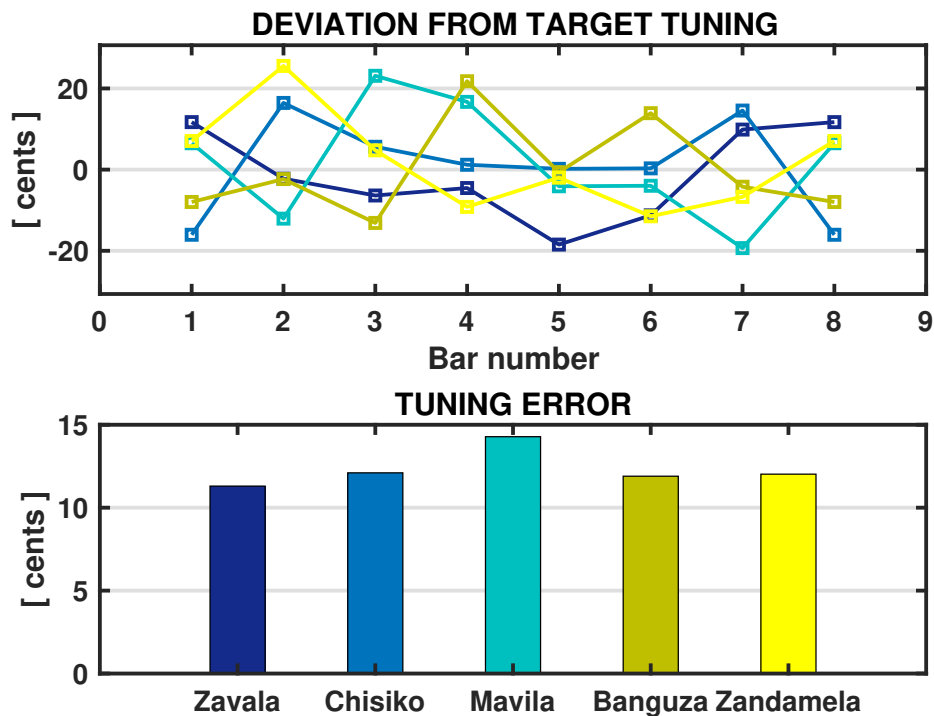| Orchestra | $f$ (Hz) | $f^\star$ (Hz) | Difference (cents) |
|---|---|---|---|
| Zavala | 252 | 250.3 | -11.7 |
| Chisiko | 256 | 258.4 | 16.0 |
| Mavila | 260 | 259.0 | -6.5 |
| Banguza | 260 | 261.2 | 8.0 |
| Zandamela | 276 | 274.9 | -7.0 |



**Figure 3.9:** Overall tuning errors in relation to a theoretical heptatonic scale based on the computed optimal reference frequency for the instruments studied by Tracey (Tracey, H., 1948).

## 3.4  Previous work on acoustic characterization of timbilas

Scientific interest in timbilas has risen in the past decade, and particularly, the collection of the National Museum of Ethnology has been of curiosity for several researchers through the past years. Luis Henrique (Henrique, L., 2004) studied the tuning of one of those instruments – a 12 bar *Dole* timbila – for his PhD thesis about bar instruments. Henrique performed acoustic measurements and vibrational experiments by impact testing, using a hammer and accelerometer, presenting a modal analysis of the bars and an analysis of the musical intervals. The researcher, however, faced certain limitations on his measurements due to the restrictions imposed to preserve the historical instruments:

> In the tests of traditional instruments of the National Museum of Ethnology, it was sometimes quite difficult to identify some modes of the bars, due to the fact that the disassembly of the instrument bars was not authorized, a fundamental condition to carry out a rigorous modal identification. Thus, in some cases there are several measures that are "contaminated" with parasitic resonances, corresponding vibrations from adjacent bars, or from the structure (Henrique, L., 2004, pg. 85).

Ten years later, the researcher and xylophone maker Nikolaus Warneke performed acoustic characterization and presented tuning measurements for the whole collection of timbilas of the National Museum of Ethnology (Warneke, N., 2014) . Although covering the complete collection, his measurements remain rather limited in terms of identifications of the instruments: attention was focused on the sounding frequency only and, apart from the value measured for each bar of the different instruments, no further analysis is attempted. However, Warneke's work appears particularly useful for future work as it provides a complete inventory of the collections stored in Portuguese museums. The inventory, presented on Figure 3.10, shows that the collection contains all five kinds of timbila, which will allow us to make acoustic characterization of the complete range of the orchestra.

| No inventaire | Nombre de lames | Nom vernaculaire | Pays /région/ville | culture | Entrée musée | Collecteur/ année | Ancien propriétaire |
|---|---|---|---|---|---|---|---|
| AA.047 | 7 | Dimbila | Moçambique/ Malia | Maconde | 1965 ? | Margot Dias | |
| AA.317 | 4 | Chikhulu | Moçambique/ Quissico | Chopi | 1965 | Margot Dias via Valente Jamine 1959 | Nyagutou |
| AA.319 | 16 | Mbingui | Moçambique/ Quissico/ Banguza | Chopi | 1965 | Margot Dias via Valente Jamine 1959 | |
| AA.321 | 11 | Debiinda | Moçambique/ Inhambane/ Guilaze-Zavala | Chopi | 1965 | Margot Dias via Valente Jamine 1959 | Samugeni |
| AA.323 | 16 | Sanje | Moçambique// Zandamela | Chopi | 1965 | Margot Dias via Valente Jamine 1959 | Jorge Machatine |
| AA.325 | 10 | Chilandzane | Moçambique// Zandamela | Chopi | 1965 | Margot Dias via Valente Jamine 1959 | |
| AA.327 | 12 | Dole | Moçambique// Zandamela | Chopi | 1965 | Margot Dias via Valente Jamine 1959 | |
| AH.636 | 14 | Txilanzane | Moçambique/ Inhambane/ Zavala | Chopi | 1968 | Mission A. Carreira 1966 | |
| AH.637 | 14 | Silanzane pl. : Txilanzane | Moçambique/ Inhambane/ Zavala | Chopi | 1968 | Mission A. Carreira 1966 | |
| AH.638 | 16 | Lanzane pl. : Txilanzane | Moçambique/ Inhambane/ Zavala | Chopi | 1968 | Mission A. Carreira 1966 | |
| AH.639 | 16 | Lanzane pl. : Txilanzane | Moçambique/ Inhambane/ Zavala | Chopi | 1968 | Mission A. Carreira 1966 | Tchambine - Macassa |
| AK.250 | 8 | [timbila] | Moçambique/ | Chopi | 1964 1969? | Agencia Geral do Ultramare | |
| AK.251 | 10 | [timbila] | Moçambique/ | Chopi | 1964 1969 ? | Agencia Geral do Ultramare | |
| BL.9681 | 10 | [malimba] | Moçambique// Maputo | [Shanga na – Ndau] | | [Pour export ?] | |
| unknown | 10 ? | [timbila] | [Moçambique] | [Chopi] | | Sur la table -laboratoire | |

**Figure 3.10:** List of the timbilas held by the National Museum of Ethnology in Lisbon (Warneke, N., 2014, pg. 06).

# Chapter 4

# Direct characterization of the acoustical behavior of timbila bars

As a first step toward the analysis of timbilas, we conducted a series of preliminary experiments based on well-established acoustical and vibrational techniques. First, a basic signal characterization of recorded samples through temporal signal, spectral and the time-frequency representations. Then, a vibrational analysis for identifying and characterizing the important resonances of the bars, namely the modal frequencies, the modal damping and mode shapes. Interests of these approaches is to provide some quick information about the acoustical and vibrational behavior of the bars and the instruments, which will be later used as a guide for the future work, and also in order to validate our development.

## 4.1   Acoustic measurements

The acoustic analysis of the timbila bars was made by recording the sound of each mbila individually and then analyzing its main temporal and spectral features using classical signal analysis tools. Recordings were performed using a Rode NT1A condenser microphone placed in the close sound field and plugged into a Berhringher Xenyx Q802 Usb audio interface connected to a PC - see Figure 4.1. Recordings were made with the software Reaper with sample rate set to 44.1kHz at 24 bits. Each mbila was struck with a mallet at three different locations: near the bar center and close to its extremities at opposite corners, to ensure high

frequency modes to develop.



**Figure 4.1:** Experimental setup for acoustic measurement.

For the signal analysis, a custom made software was developed in order to produce temporal, spectral and time-frequency representations. The analysis provides a qualitative view of how the sound is built and developed. Figure 4.2 shows the temporal signal, the spectral representation, and the time-frequency representation of a typical sound obtained experimentally. The signal duration is short, less than 1s. It starts with a very short transient which rapidly decays, and is followed by a sort of reverberation at a single frequency, reflecting the influence of the gourd resonator on the sound production. By looking at the frequency spectrum in Figure 4.2a, we notice well separated peaks at 493 Hz, 1837Hz, 2745Hz and 4050Hz. The spectral development of the partials presented on Figure 4.2b clearly shows that damping is frequency dependent, with a longer sustain for the fundamental mode while the following partials decay very quickly after the attack.

## 4.2   Experimental modal analysis

The second series of tests was to perform experimental modal analysis based on impact testing in order to identify the natural frequencies, modal damping and mode shapes of the timbila bars. Experimental modal analysis is a classical experimental procedure for determining the
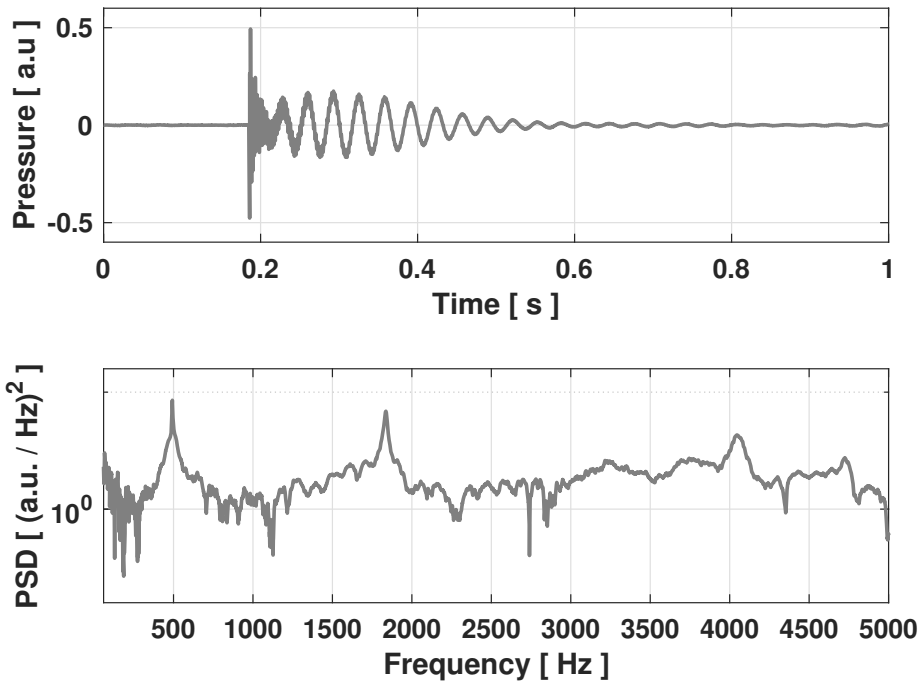
**(a)** Time domain (up) and frequency domain (bottom) representations of the recorded pressure signal.
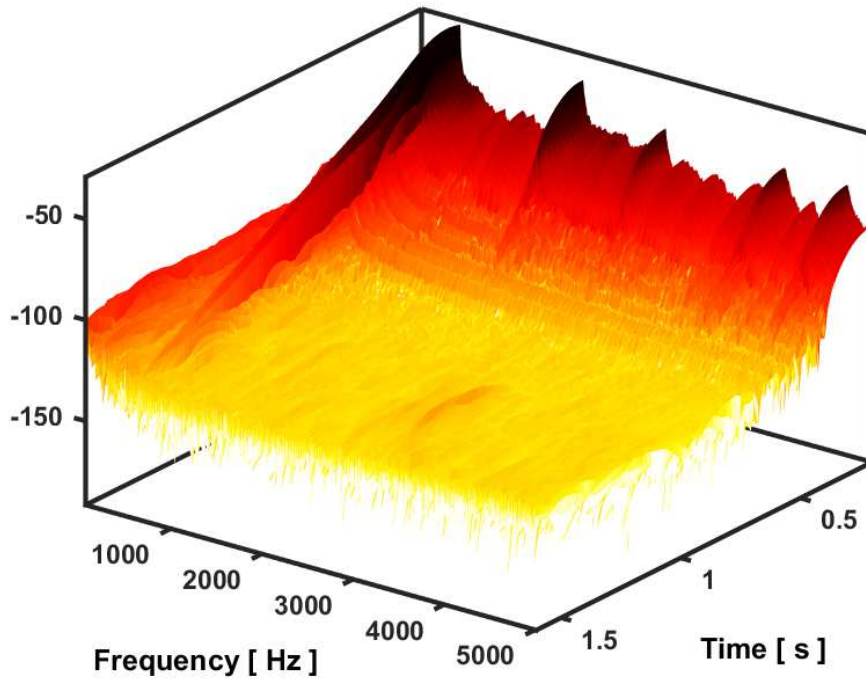


**(b)** Spectrogram of the recorded pressure signal.

**Figure 4.2:** Signal analysis of a typical sound obtained by impacting bar # 4 of the laboratory timbila.

modal parameters of complex vibrating structures, including musical instruments (Fu, Z.F. and He, J., 2001; Fletcher, N. H. and Rossing, T. D., 1998; Bork, I. et al., 1999), and results will be used as a reference to validate the method developed in this dissertation.

## 4.2.1   Impact testing

For such experiment, an impact hammer instrumented with a force sensor is used to provide some input vibrational energy to the bars while other sensor is used to measure their vibrational responses.   In this work, we attempt two different approaches, using first a piezoelectric accelerometer glued to the bar and second a digital laser vibrometer pointed at the bar.  If the two types of sensors actually measure different physical quantities, the most important difference remains in the fact that laser sensing technology allows contactless measurements, which are clearly more appropriate for objects found in museums' collections.

We first conducted the impact test experiment using the accelerometer (Figure 4.3). The impact hammer was used to strike three points in the structure while the piezoelectric accelerometer, glued to the bar with wax, measured the response. Excitation was performed using a PCB 086E80 impact hammer equipped with a rubber head. The vibratory responses were measured using a Brüel & Kjaer 4375 accelerometer connected to a charge amplifier Brüel & Kjaer 2635. The accelerometer was placed near one corner of the bar, in a position adequate to obtain a vibrational response including bending and torsion modes. Signals were recorded at a sampling frequency of 12600 Hz and pre-processed by using the multi-channel data acquisition system Siglab 20-42 in order to compute impulse responses and transfer functions. The length of the signals was about 0.6 s, which seems a good compromise for recording the full decay of the bar vibration. Measurements using the laser vibrometer were then performed similarly. For each type of experiments, three measurements were performed, by striking opposite ends and the center of the bars. For illustration, typical examples of the measured input force and velocity responses are plotted in Figure 4.4.

A quick analysis of the measured transfer function on the Siglab acquisition system software reveals some discrepancies between the two types of experiments (see Table 4.1). Errors in modal frequencies are found to be up to 7%, which is not acceptable but easily understandable. The reason is due to the added-mass effect of the accelerometer glued to the bars, which perturbs its natural vibrations and lowers all the modal frequencies.  Moreover,

**Figure 4.3:** Experimental setup with impact hammer and accelerometer.
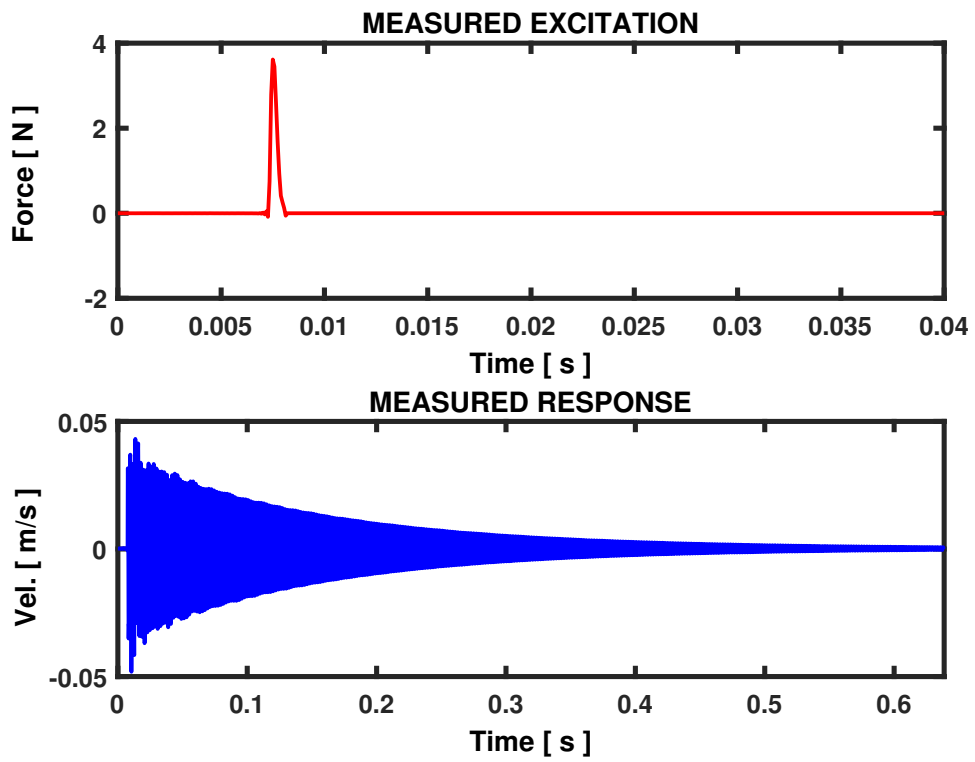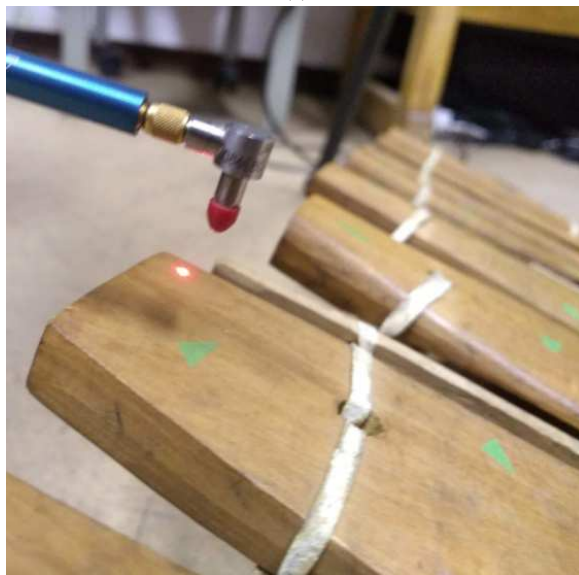


**Figure 4.4:** Typical examples of measured excitation force and vibratory response using the laser vibrometer.

(a)


(b)

**Figure 4.5:** Experimental setup for vibrometer laser measurements.

we notice a reasonable good agreement between the frequency values of the main resonance stemming from acoustic and laser measurements, thus highlighting the necessity of using contactless measurement techniques for performing the vibrational characterization of timbila bars (see Table 4.2).

| | BAR# | ACC (Hz) | LASER (Hz) | DEV (%) |
|---|---|---|---|---|
| | 1 | 359,37 | 373,59 | 3,81 |
| | 2 | 393,75 | 408,37 | 3,58 |
| | 3 | 431,25 | 443,99 | 2,87 |
| F1 | 4 | 478,12 | 493,39 | 3,09 |
| MODES | 5 | 528,12 | 546,74 | 3,41 |
| | 6 | 578,12 | 607,7 | 4,87 |
| | 7 | 628,12 | 668,16 | 5,99 |
| | 8 | 690,62 | 739,15 | 6,57 |
| | 9 | 762,5 | 812,78 | 6,19 |

**Table 4.1:** Comparison between f1 modes identified on both accelerometer and laser experiments

| | | MEASUREMENTS (HZ) | | | DEVIATION (%) | |
|---|---|---|---|---|---|---|
| | BAR# | SPECTRUM | ACC. | LASER | ACC. | LASER |
| | 1 | 372,5 | 359,37 | 373,59 | 3,52 | -0,29 |
| | 2 | 407,5 | 393,75 | 408,37 | 3,37 | -0,21 |
| | 3 | 443,1 | 431,25 | 443,99 | 2,67 | -0,20 |
| F1 | 4 | 492,5 | 478,12 | 493,39 | 2,92 | -0,18 |
| MODES | 5 | 546,2 | 528,12 | 546,74 | 3,31 | -0,10 |
| | 6 | 606,45 | 578,12 | 607,7 | 4,67 | -0,21 |
| | 7 | 667 | 628,12 | 668,16 | 5,83 | -0,17 |
| | 8 | 737,7 | 690,62 | 739,15 | 6,38 | -0,20 |
| | 9 | 811,8 | 762,5 | 812,78 | 6,07 | -0,12 |

**Table 4.2:** Deviation of each vibrational measurement method (accelerometer and laser) in relation to the acoustic measurements of F1 modes.

## 4.2.2 Modal identification

To quantify more precisely the modal frequencies and estimate the modal damping of each bar, modal identification was performed with an implementation of the Eigensystem Realization Algorithm (ERA) (Juang, J., 1994) using recorded signals from the impact hammer and the laser vibrometer. Each bar transfer functions and corresponding impulse

responses were computed and objective of the algorithm is to provide the adequate set of modal parameters that best-fit the measured impulse responses. Retaining a modal representation for describing the linear dynamical behavior of the bar, the impulsive response $h(\mathbf{r_e}, \mathbf{r}, t)$ measured at location $\mathbf{r}$ for an excitation given at location $\mathbf{r_e}$ can be expressed as a sum of damped modal responses, following the form:

$$h(\mathbf{r_e}, \mathbf{r}, t) = \sum_{n=0}^{N} A_n(\mathbf{r_e}, \mathbf{r}) e^{-\omega_n \zeta_n t} \sin(\omega_n \sqrt{1 - \zeta_n^2}\, t) \tag{4.1}$$

where $A_n(\mathbf{r_e}, \mathbf{r})$ represents the modal amplitude of mode $n$, and $\omega_n = 2\pi f_n$ and $\zeta_n$ are the modal frequency and modal damping associated with mode $n$ respectively. By Fourier transforming Eq.(4.1), we obtain the transfer function, which reads as:

$$H(\mathbf{r_e}, \mathbf{r}, \omega) = \sum_{n=0}^{N} \frac{A_n(\mathbf{r_e}, \mathbf{r})}{\omega_n^2 - \omega + j2\omega\omega_n\zeta_n} \tag{4.2}$$

where now $\omega = 2\pi f$ is the frequency variable and $j$ is a complex number ($j^2 = -1$).

In practice, modal identification was achieved using three measured impulse responses. Figure 4.6 shows an example of an impulse response and its transfer function measured on bar # 4, together with the reconstructed functions using the identified modal parameters, showing that the estimation was reliable up to 5000 Hz. Table 4.3 finally lists the results of our modal identifications for each mbila.

We can then analyze the tuning of the bar overtones by looking at the ratios between the modal frequencies between each mode in relation to the first one. As can be seen in Figure 4.7, results show a great variability along the musical scale of the instrument, although similar calculations would result in more consistent values for a marimba bar (Beaton, D. and Scavone, G., 2019). From the point of view of pitch perception, the main drawback of this result is that the pitch is not as clearly defined as in the case of an harmonic spectrum because higher partials do not share any temporal periodicity with the fundamental frequency.

As anticipated for wooden bars (Chaigne, A. and Doutaut, V., 1996), damping is found frequency-dependent, increasing with the frequency. Notably, the damping for the second mode, which in fact corresponds to torsional motion, is large compared to the other modes. One possible reason is the influence of the suspending cord on the mode shape, which

may damp motion at the locations of the cord on the bar although the bar would significantly vibrate if it was free. Notably, this trend can also be seen in the results for the historical timbila measured by Henrique (Henrique, L., 2004), where the identified modal damping values for torsional modes are in the range 1-2%, with larger values found for the first torsional modes.
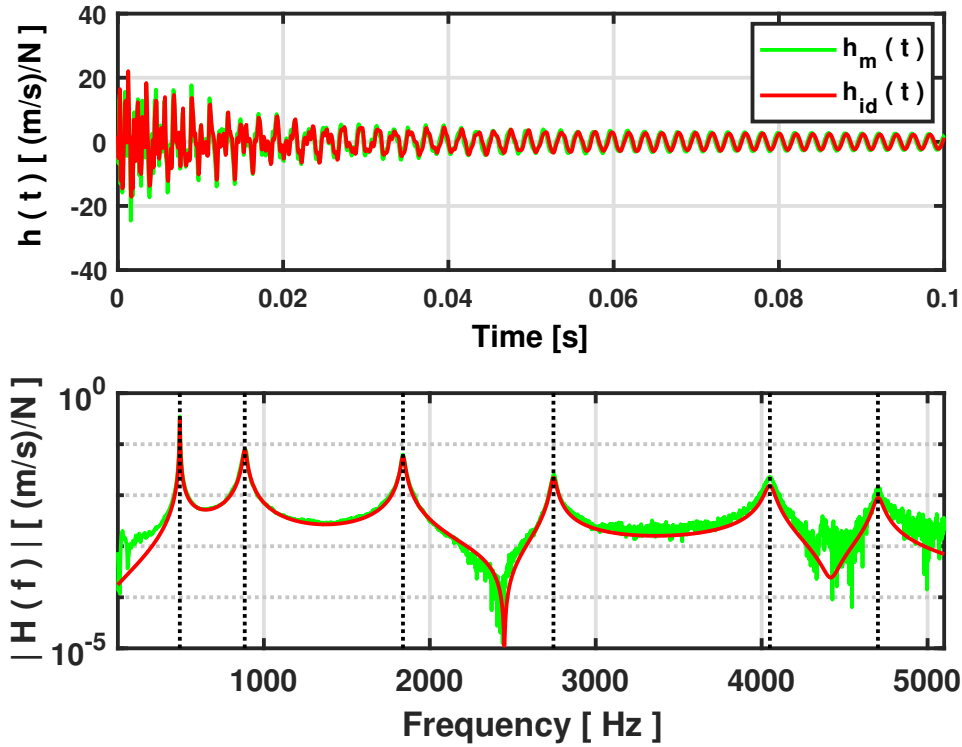


**Figure 4.6:** Comparison between measured and synthesized impulse functions (top) and transfer functions (bottom) for bar # 4. Vertical dotted gray lines stand for the identified modal frequencies.

We also performed a full experimental modal identification of one bar of the laboratory timbila in order to identify the mode shapes. In the experiment, impact excitations were given at 53 regularly spaced points on the bar - see Figure 4.8, while the vibrational responses were measured at a single point, close to a bar corner, using the laser vibrometer. The modal identification was then performed using the set of 53 computed impulse responses. Results are presented in Figures 4.9-4.13, where it can be seen that modes alternate between bending ($f_1$, $f_3$, $f_5$) and torsional ($f_2$, $f_4$) motion, as commonly observed for vibraphone/marimba bars and in a similar manner to measurements by Henrique (Henrique, L., 2004).

The fundamental mode is a pure bending mode with two nodal lines that are close to the locations of the hole and the supporting cord, which are displayed in black

41

| | | Frequency (Hz) | Damping (%) |
|---|---|---|---|
| BAR 1 | f1 | 373,59 | 0,335 |
| | f2 | 724,16 | 3,041 |
| | f3 | 1560,16 | 0,331 |
| | f4 | 2508,82 | 0,507 |
| | f5 | 3605,03 | 0,464 |
| BAR 2 | f1 | 408,37 | 0,241 |
| | f2 | 767,93 | 1,299 |
| | f3 | 1649,57 | 0,297 |
| | f4 | 2583,15 | 0,589 |
| | f5 | 3728,21 | 0,857 |
| BAR 3 | f1 | 443,99 | 0,194 |
| | f2 | 771,87 | 1,101 |
| | f3 | 1683,4 | 0,253 |
| | f4 | 2474,97 | 0,516 |
| | f5 | 3775,95 | 0,597 |
| BAR 4 | f1 | 493,39 | 0,273 |
| | f2 | 886,79 | 1,81 |
| | f3 | 1837,63 | 0,337 |
| | f4 | 2746,8 | 0,654 |
| | f5 | 4050,72 | 0,668 |
| BAR 5 | f1 | 546,74 | 0,294 |
| | f2 | 943,79 | 1,482 |
| | f3 | 2102,21 | 0,414 |
| | f4 | 3099,29 | 0,504 |
| | f5 | 4592,28 | 0,536 |

| | | Frequency (Hz) | Damping (%) |
|---|---|---|---|
| BAR 6 | f1 | 607,7 | 0,25 |
| | f2 | 1345,48 | 1,498 |
| | f3 | 2259,47 | 0,412 |
| | f4 | 3587,66 | 0,498 |
| | f5 | 4652,94 | 0,648 |
| BAR 7 | f1 | 668,16 | 0,207 |
| | f2 | 1405,3 | 2,575 |
| | f3 | 2318,21 | 0,389 |
| | f4 | 3429,64 | 0,472 |
| | f5 | 4787,27 | 0,552 |
| BAR 8 | f1 | 739,15 | 0,249 |
| | f2 | 1598,23 | 1,881 |
| | f3 | 2528,73 | 0,612 |
| | f4 | 3821,23 | 1,052 |
| | f5 | 5070,33 | 0,781 |
| BAR 9 | f1 | 812,78 | 0,224 |
| | f2 | 1764,9 | 1,345 |
| | f3 | 2799,55 | 0,549 |
| | f4 | 4103,39 | 0,591 |
| | f5 | 5757,35 | 0,758 |

**Table 4.3:** First five experimentally identified modal frequencies and modal damping values of each mbila.
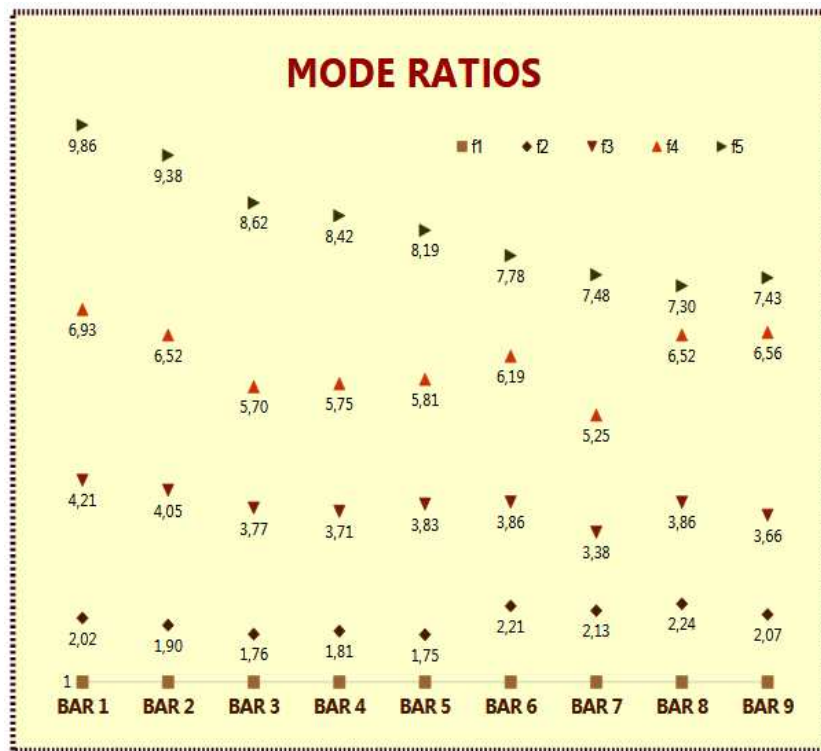
**Figure 4.7:** Frequency ratios of the five first modes in relation to the first mode.

on Figures 4.9-4.13. As well known by makers, these two near-zero vibration areas are particularly adequate for positioning the supporting cord. The second mode shows a rotation around the longitudinal axis, with two perpendicular nodal lines, thus being the first torsional mode. As already mentioned, this mode has high damping and, because it shows symmetric displacement areas moving in opposite phases, does not radiate significantly. Indeed, it cannot be seen in the spectrum of Figure 4.2a. The third mode is again a bending mode, with three nodal lines, one of them in the middle of the bar, which means this partial will not appear in the radiated spectrum when the bar is struck at the bar centre. The fourth mode is the second torsional mode and the fifth mode is the third bending mode, with a maximum motion amplitude at the centre, contrary to the third mode. Clearly, this shows the relevance of the impact location in determining which modes will participate in the vibration and respective sound.

Globally, these experiments provide a first characterization of the instrument that allows some understanding about the musical features of this specific timbila. However, performing a full modal analysis of all the bars comprising the instrument could be time-consuming, particularly if several instruments demands such systematic analysis. Moreover, analyzing the tuning of the overtones is not an easy task since the modal density increases

43

with the frequency, leading to uncertainties for assigning one identified mode to a specific motion.



**Figure 4.8:** Experimental mesh for the complete modal analysis of bar # 4. The laser was pointed to the top left corner and impacts were given at all marked points of the mesh.
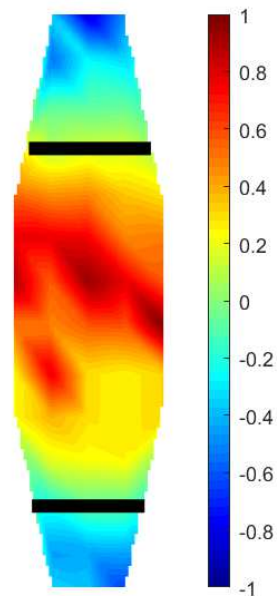


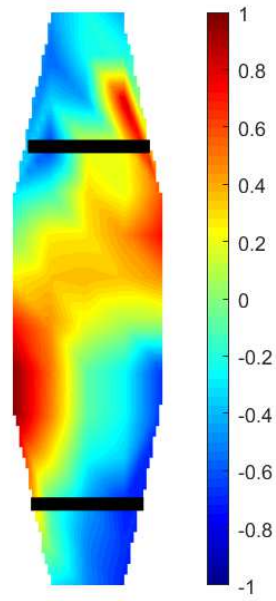**Figure 4.9:** First experimentally identified mode shape. Bar # 4.

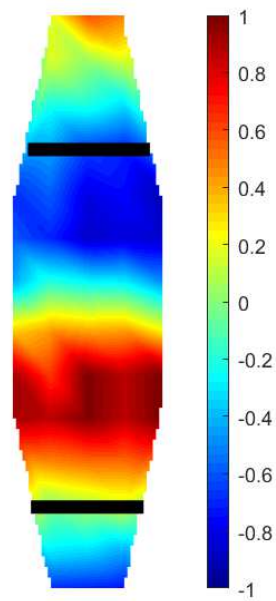**Figure 4.10:** Second experimentally identified mode shape. Bar # 4.
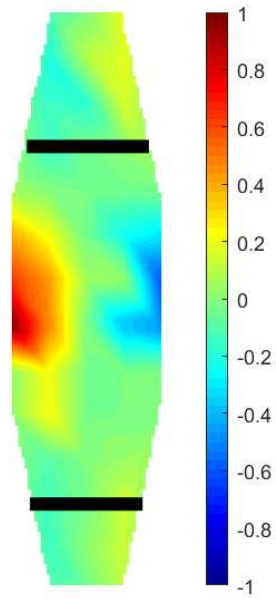


**Figure 4.11:** Third experimentally identified mode shape. Bar # 4.

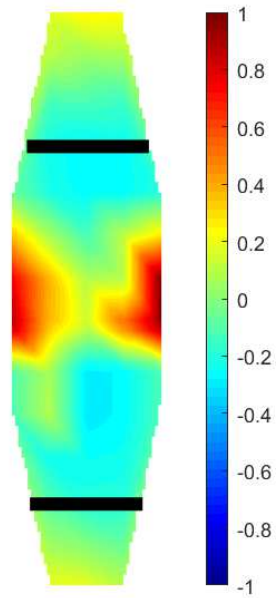Figure 4.12: Fourth experimentally identified mode shape. Bar # 4.



Figure 4.13: Fifth experimentally identified mode shape. Bar # 4.

# Chapter 5

# Reverse-engineering procedure for the characterization of timbila bars

For this dissertation, we devised an alternative technique for the characterization of bar instruments, employing a careful methodology based on sophisticated non-intrusive reverse engineering techniques. Research has demonstrated the power and efficiency of shared methodologies, and analysis techniques of acoustics have proven to be insightful for acousticians and musicologists. They can objectively explain the sonority of instruments (Fletcher, N. H. and Rossing, T. D., 1998), guide conversation protocols (Conte, S. L. et al., 1999), resurrect the sound of musical artifacts (Debut, V. et al., 2016b) and provide relevant insights on musical structure, practice and instrument making (Debut:05, Debut:10b, Debut:16a).

In 1992, a multidisciplinary team undertook the reconstruction of the carnyx, an ancient Celt instrument. To evaluate the success of a copy designed on the basis of artifacts and representations, resonance and playing frequencies of the instrument were analysed by experiments and computer simulations (Campbell, M. and Kenny, J., 2012). In 2002, IRCAM (Institute for Research and Coordination in Acoustics based in Paris) developed a computer model of a flute as part of a collaboration project with ethnomusicologists (Cuadra, de la, P. et al., 2002). Objective was to understand the musical scale used by flutists from Cameroon. The use of a virtual model enabled a precise analysis of the tuning.

The same team which conducts *Music research and new technologies towards the restitution of the timbila collection of the National Museum of Ethnology* has previously devised strategies to assess the tuning properties of carillons. The approach combined vibration analysis with math-based optimization strategies (Debut, V. et al., 2016a), and was successfully applied to the Mafra's carillons, objectively providing musicological insights. In collaboration with a group expert in material science, these researchers also asserted the tuning properties of the oldest bell in Portugal (Debut, V. et al., 2016b). Combining elemental and micro-structural analysis, non-destructive measurements and computer modeling techniques, the work enabled to rediscover the sound of this unique broken bell.

Based on a similar methodology, we are able to approach the timbila in a new and original way. The proposed approach combines non-invasive up-to-date imaging technology with modelling and computational techniques from vibration analysis, and can be summarized in the following steps:

1. to perform a precise assessment of the bar geometry using 3D scanning technology;

2. to built a Finite Element Model of the bar from the scanned data;

3. to assert the bar modal properties by modal computations and analyze its tuning.

## 5.1   Geometry assessment

The 3D scan imaging technology combines sophisticated techniques of image acquisition with processing algorithms and enables to assess the geometry of intricate objects in a fast and detailed manner. This technology allows high resolution assessment of the geometry with the advantages of the method being non-destructive and non-invasive, following the rules of preservation of museum objects. In this work we used the Artec Eva 3D handheld scanner - see Figure 5.1, which consists of one projector and two cameras that capture and simultaneously process up to two million geometrical points per second, with an overall dimensional tolerance of 0.5 mm. The scanner takes a sequence of images with different patterns of LED light projected onto the surface of the object. Interestingly, it also captures the colors of the objects, which can be then used to generate a texture for the final full

3D rendering model. Basically, the complete process of scanning includes the following stages:(a) scanning; (b) aligning; (c) cleaning, and (d) rendering.



**Figure 5.1:** The Artec Eva 3D scanner.

### 5.1.1 Scanning

The bars are scanned by sweeping the device along the timbila from a distance of 40cm to 1m, capturing 3D frames from the surface pointed by the scanner. We decided that scanning could be done sequentially around sections of two or three bars at a time and then treat each bar individually. The procedure was then repeated for the neighboring sections of bars, until all the bars comprising the instrument were captured. Scanning must be done with special care and can take a few hours to be accomplished. To improve the signal-to-noise ratio of the images, scanning must be performed perpendicular to the surface, thus imposing to scan the object from different angles and positions. Depending of the complexity of the shape of the object, some areas require special attention to be captured correctly. For instance, scanning the bottom of the bars was particularly challenging due to the small distance between the bar and the resonator (see Figure 3.3). As a result, this often leads to very noisy data that must be processed carefully at later stage.

### 5.1.2 Aligning

In general, several scans are needed to capture the complete surface of a bar and the corresponding raw data consists of unorganized images, sometimes including unwanted parts

of the object (see Figure 5.2). Therefore, the first step of the post processing is to align the series of different scans that have been captured. This is achieved by selecting manually reference points on pairs of scans, which are then linked and collapsed, resulting in aligned scans. For that matter, before the scanning, we glued colored stickers with geometrical forms to the bars, to be used as reference on aligning. The most difficult step on this stage is to align scans from opposite faces, which requires "transition" scans that capture both sides and are then used to align all the other scans in order to reconstruct the 3D geometry.
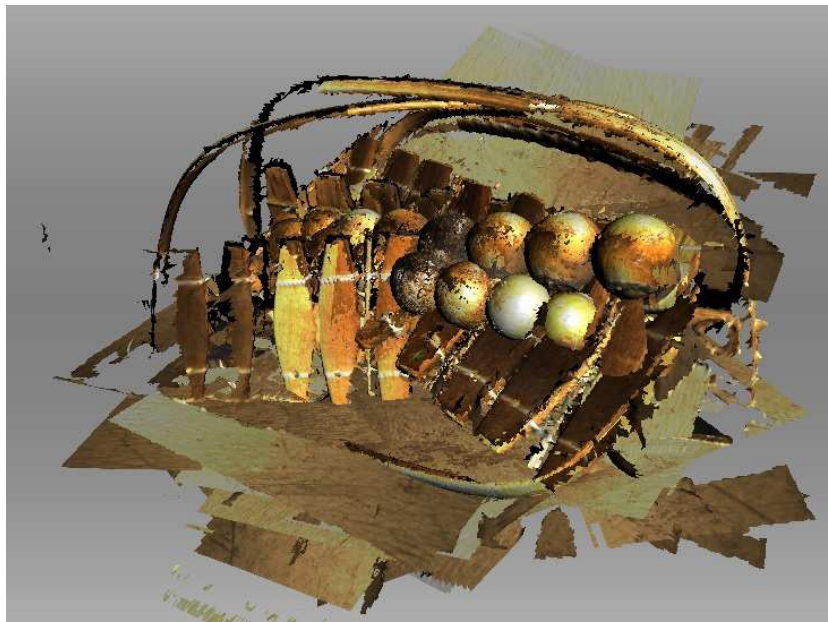


**Figure 5.2:** Unaligned raw data from several scans of the laboratory timbila.

### 5.1.3 Cleaning

Of course, the scans do not capture exclusively the desired geometry but also include data of the surrounding objects and background, which are unwanted material. Deleting such noise is thus required in order to produce the relevant surfaces of the scanned object. Cleaning is therefore another essential step which must be done carefully, in particular close to the edges of the object. In practice, we spent a lot of time on this task, which can take up to six hours in order to get a well cleaned isolated bar (Figure 5.4).

### 5.1.4 Rendering

There is further steps of post-processing for surface reconstruction before consolidating the complete 3D model and obtaining the full rendering. After manual alignment and cleaning,
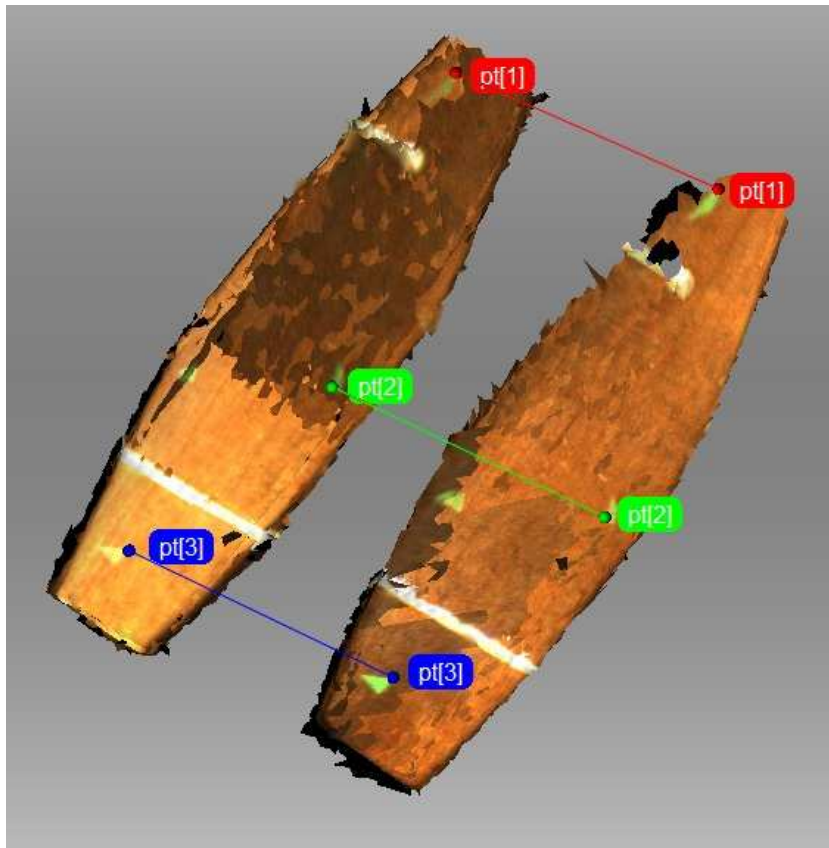
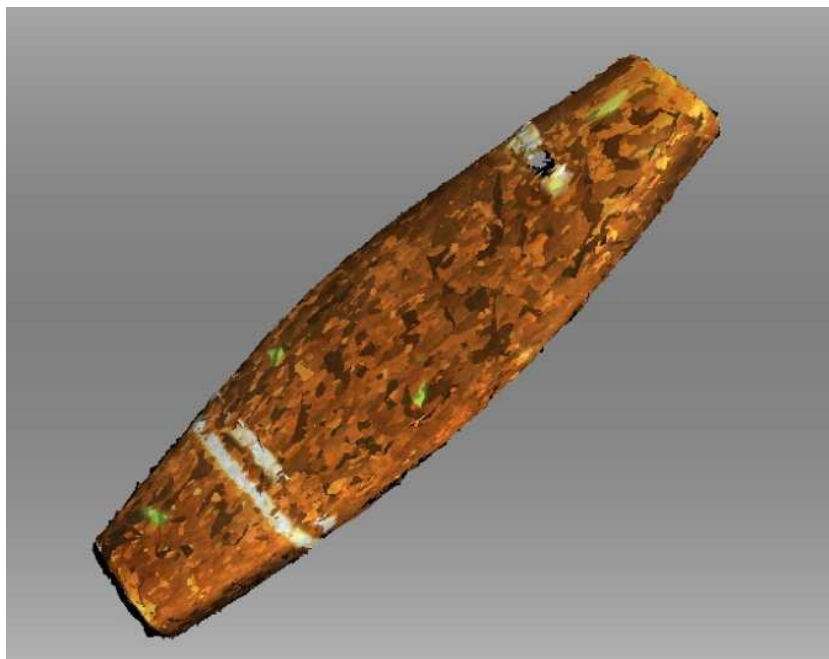**Figure 5.3:** Alignment process between two scans.



**Figure 5.4:** Bar # 4 after cleaning stage and before rendering.

the global-registration algorithm converts all one-frame surfaces to a single coordinate system using information on the mutual position of each surface pair. Last stage to consolidate the geometry is the fusion, a process that creates a polygonal 3D model by melting and solidifying the captured and processed frames. This finally results in a 3D surface mesh. We can also opt to give the geometry a texture treatment, a finishing layer that applies the colors of the objects. This will not affect the geometry, being for purely aesthetic purposes. We now have the final 3D model, as plotted in Figure 5.6.



**Figure 5.5:** Final 3D colored rendering for bar # 4.

### 5.1.5   Exporting mesh

The final 3D surface mesh (Figure 5.6) can be finally exported as a discrete surface modeled using simplified polygons. The file format that has been retained is STL, an abbreviation of"stereolithograph", which is one of the standards for 3D objects and is supported by many CAD softwares (Szilvasi-Nagy, M. and Matyasi, G., 2003).

**Figure 5.6:** Final surface mesh.

## 5.2　Finite Element modeling and modal computation

Finite Element Method (FEM) is a modeling technique widely used in the industry for solving different types of engineering problems, including the prediction of the vibrational behavior of complex mechanical structures. The vibratory behavior of any structure can be described mathematically by partial differential equations (Multiphysics cyclopedia, 2016), which usually cannot be solved exactly except for rather simple structures. The FEM approach provides an approximation of the solution by discretizing the structure into a number of small elements and connecting them according to adequate mathematical relationships between neighboring elements. The discrete elements are connected at nodes (Figure 5.7), as if nodes were pins or drops of glue that hold elements together (de Weck, O. Y. and Kim, I. Y., 2004).



**Figure 5.7:** The timbila bar is divided into a number of elements connected by nodes.

Within the scope of this work, the FEM technique is used to investigate the

53

dynamical behavior of the bars of the instrument by performing modal computations in order to calculate the frequencies and the vibratory forms of the main resonances, which in turn allows to analyze the tuning and musical scales of the instrument.

## 5.2.1    Building the FEM model

Before performing computations, the procedure starts with the transformation of the *surface* mesh stemming from the scanning process into a *solid* mesh, with its respective volume. The discrete elements are simple geometrical shapes, usually triangles, quadrilaterals, tetrahedrons or hexagons (Tabatabaian, M., 2014).    For our computations, bars were discretized using 10-node tetrahedron elements resulting in a solid mesh as illustrated in Figure 5.8.
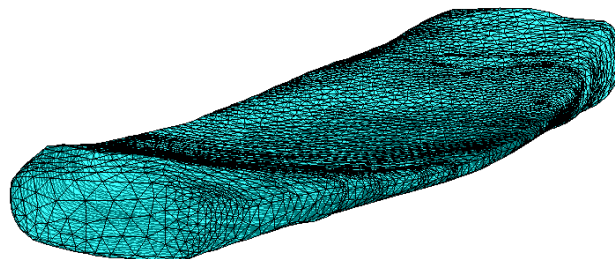


**Figure 5.8:** Example of a solid mesh of one of the timbila bar, built using tetrahedron elements.

The accuracy of the physical model and the associated computations depends on the level of details and accuracy of the model, and the type and number of elements used for the volume discretization need to be sufficiently large in order to precisely describe the structure geometry.  Choosing the size and number of elements for building the mesh is problem dependent and must be asserted by systematic tests of convergence of the computation for increasing values of numbers of elements.

### 5.2.2 Material mechanical properties

The second fundamental ingredient for performing any vibration analysis is to know the mechanical properties of the material of the structure, given through values of its density, modulus of elasticity and Poisson's ratio. The selection of these parameters is in many cases straightforward for common materials for which information is tabulated in the literature. However, wood material properties, in particular for specific wood, are generally scarce. One inherent difficulty in wood mechanics is due to its orthotropic nature, a kind of anisotropy in which properties differ along the main directions and that ultimately makes mechanical modeling delicate (Green, D. W. et al., 1999). Instead of three parameters that are needed for describing isotropic material, a set of nine parameters is necessary for accurate modeling of wooden bars: three moduli of elasticity (Young's moduli), three moduli of rigidity (shear moduli) and three Poisson's ratios (Bork, I. et al., 1999).

If wood databases usually present properties in the direction parallel to the fiber, they are however not extensive for both the radial and tangential directions, and this is the reason to explain why many music acoustics studies concerned with wooden percussion instruments usually modeled wood as isotropic material (Bork, I. et al., 1999; Chaigne, A. and Doutaut, V., 1996; Aramaki, M. et al., 2007). This obviously remains an approximation of the real physics and limits the validity of the FE modeling. However, it must be noticed that the ratio length/width for musical bar is usually large and that bars are also cut in the longitudinal direction, so that using the longitudinal properties remains a first valid approximation for vibrational analysis. Quantitatively, Bork et al. (Bork, I. et al., 1999) noticed that, for marimba bars, using an isotropic FE modeling was efficient in predicting the frequencies and mode shapes of the first three vertical bending modes, but led to large errors for higher-order modes and torsional modes.

### 5.2.3 Modal computations

A central topic in mechanical vibrations, and more specifically in the analysis of periodic motion, is the computation of the natural vibrational properties of flexible structures, namely the modal parameters. The problem is common in practice in many fields of engineering and of particular interest in music acoustics in order to predict the tuning of musical instruments (Debut, V. et al., 2005, 2016a). Technically, the problem consists of calculating the solutions

of an eigenvalue problem and thus finding the eigenvalues and corresponding eigenvectors, from which the natural frequencies and motions of the structure can be predicted. In this work, computing eigenvalues from the FE model is central in order to compute the modal parameters of the bar. It involves a fair amount of manipulative details - see (Linz, P. and Wang, R., 2003), for instance -, but computer programs are readily available, so the need for implementing them does not arise.

# Chapter 6

# Application of the techniques to the timbila and physics-based sound synthesis

We finally present the results stemming from the methodology developed through this dissertation. We start by illustrating the potential of the technique to provide a detailed analysis of the geometry of bars, thus demonstrating one of the most interesting direct possibilities offered by 3D scanning technology. Modal computation results will then follow, by presenting a modal analysis of the bars from the FE models built from the scan data and by comparing the results with values obtained experimentally. Finally, we will present other possible output from the computed data, proposing a physics-based approach to sound synthesis of timbila bars in order to, in future, recreate the sound of the instrument virtually.

## 6.1   Systematic geometry analysis

As an illustration, a detailed analysis of the geometry of bar # 4 of the laboratory timbila is now made using the complete 3D model, by focusing on its typical dimensions, its volume and an analysis of the shape of the undercut, which is fundamental for tuning bar instruments.

The volume of the bar can be first calculated from the vertices of the triangles[1] that are used to approximate the surface of the object using the formula (Zhang, C. and Tsuhan,

---

[1]A vertex is the coordinates of the corner of the triangles which approximates the geometry of the object.

C., 2001):

$$V = \frac{1}{6} \sum_{i=1}^{N} \mathbf{v}_{i1} \cdot \left[ (\mathbf{v}_{i2} - \mathbf{v}_{i1}) \otimes (\mathbf{v}_{i2} - \mathbf{v}_{i1}) \right] \qquad (6.1)$$

where $\mathbf{v}_{ij}$ is the vector of the vertex $j$ that from the origin that defines triangle $i$. Knowing the density of the material $\rho$, the mass of the object is straightforward, given by $m = \rho V$. For the studied bar, the volume was found to be of the order of 8.3 $10^{-5}$ m$^3$, resulting in a mass of 83 gr if ones assumes the density of 1000 kg/m$^3$ for the wood species *Mwenje*.

The 3D model can be then converted into a series of slices that are closed contours representing the cross sections of the bar along a specific direction. In our context, this provides a way of studying the variation of thickness of the bars along their lengths, which is known to be crucial for tuning. Interestingly, these data can be also used for directly copying original bars through 3D printing, which is a manufacturing technique that is actually based on 2D adding layer process that required slices as inputs.

In this work, we successfully developed a basic slicing algorithm in order to systematically produce contour data from the STL files of the bars. For a given plane of intersection, the algorithm intersects all triangles of the surface with the plane and then links the resulting line segments by simple head-to-tail rule, which finally results in a closed polygon. The algorithm was built for a constant spacing between successive planes, defined by the user, and requires STL files free of errors. Indeed, when approximating a geometry by a triangulated surface, errors can frequently arise due to a fault in the conversion, including holes in the mesh or the presence of overlapping triangles. This therefore demands to fix errors in the STL file before performing any post-processing, using for instance the open-source 3D computer graphics softwares *Blender*[2] or *Meshlab* [3]. Also, before performing any post-processing, other important practical aspect is to correctly align the object within a specific system of coordinates and position the center of origin according to the center of mass of the object.

For illustration, Figures 6.1 show a typical example of 3D contour image, together with the corresponding side and top views, obtained using the developed slicing algorithm. A first quick analysis reveals that the bar is 20 cm-long, with both variable width and cross-

---

[2]See https://www.blender.org/
[3]See https://www.meshlab.net/

section along its length. Interestingly, these data can be also split into separate cross-section areas as displayed in Figures 6.2. This then provides a more detailed analysis of the width and undercut of the bar and highlights how the material is removed by the maker during the tuning process. This data can be further used to study quantitatively the changes in width and area of cross-section of the bar and thus to relate changes in width with changes in cross-section along the bar length as plotted in Figure 6.3. Needless to say, obtaining such precise data for a surface with many irregularities would be very challenging through classical geometrical measurement techniques.
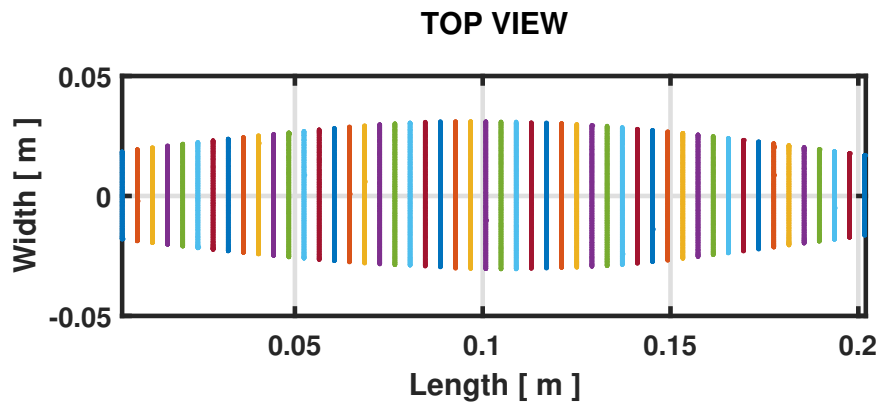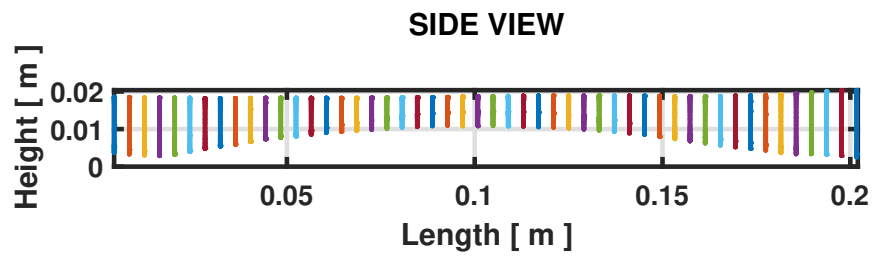
## 6.2 Modal computations

From the knowledge of the geometry of the bars, solid 3D models can be then constructed by means of Finite Elements. The *Partial Differential Equation Toolbox* of Matlab, which allows to import 3D geometries from STL files, was used to construct the FEM model as well as to carry out the numerical modal computation. For building the mesh, the selected elements were tetrahedrons with 10 nodes. While the number varies with the dimensions of the bar, systematic tests show that a total number of about 30000 elements leads to a relative accuracy of a few percent as plotted in Figure 6.4.

As mentioned in Section 5.2.2, a practical problem of our FE simulations was the selection of the constants that describe the elastic behavior of the wood, i.e. the Young's modulus, Poisson's ratios and shear moduli. Information about the species *Mwenje* is rare in the literature and only wood properties in the longitudinal direction were actually found. Computations were therefore performed assuming that bars are homogeneous and isotropic, and using average values found in the literature (Ressources, 2020). If some model updating could be attempted by adjusting the bar density and Young's modulus to modal frequencies identified experimentally, we preferred to perform computations without a precise knowledge of the wood properties, similarly to what it would be for instruments held in a museum. We therefore set the Young's modulus to its longitudinal modulus value, which was assumed to be 17.7 GPa, the density to 1000 kg/m$^3$ and the Poisson ratio to 0.3 (see Table 6.1). Also, for simplicity, modal computations were performed assuming free boundary conditions for the bars while in reality bars are fixed with straps to the supporting structure.

**3D VIEW**

(a)

**SIDE VIEW**
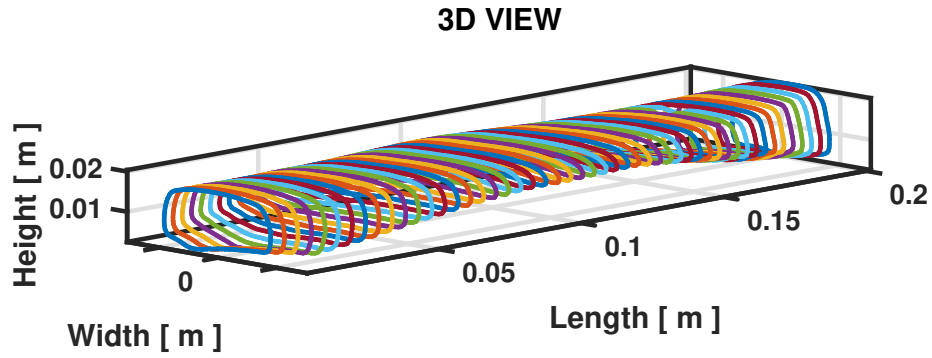
**TOP VIEW**

(b)

**Figure 6.1:** Computed slices of the geometry of bar # 4. (a) 3D view; (b) side and top views.

**Table 6.1:** Mechanical properties used for the FE modal computations.

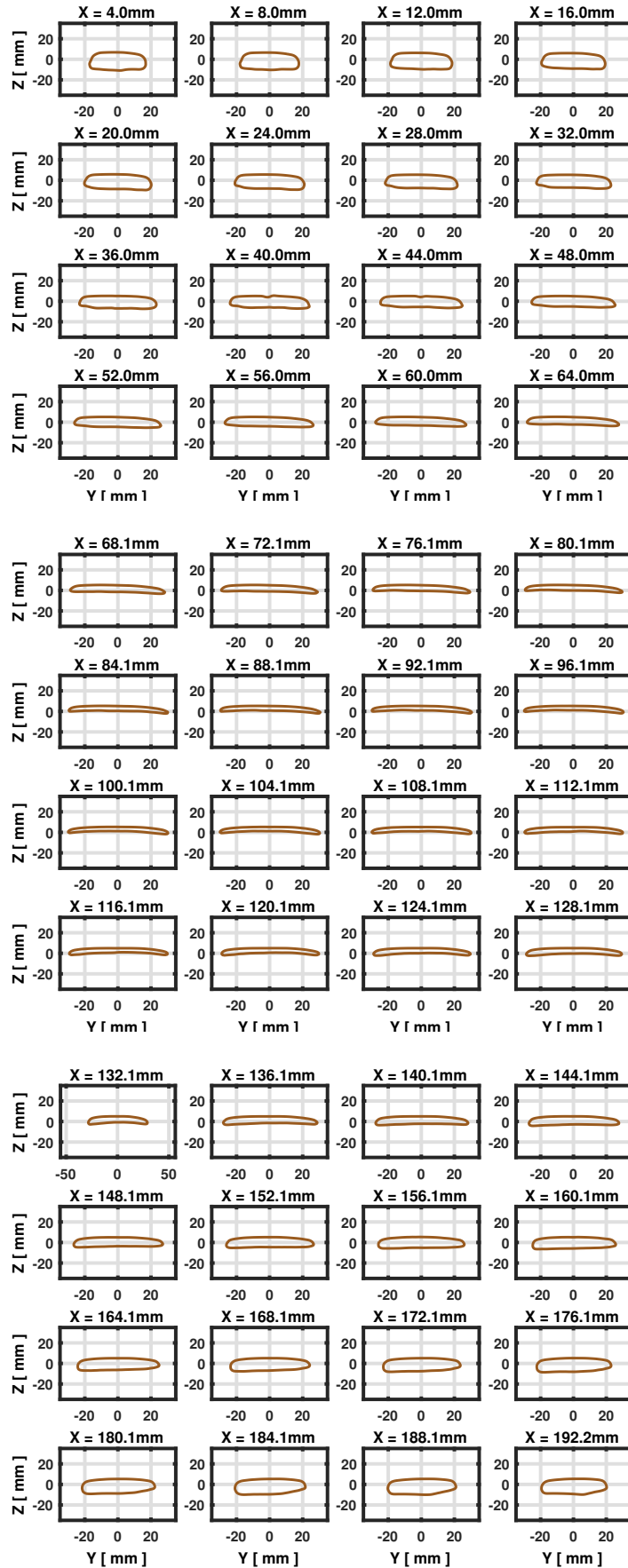| Young's modulus (GPa) | Density (kg/m$^3$) | Poisson's ratio |
|:---:|:---:|:---:|
| 17.7 | 1000 | 0.3 |

**Figure 6.2:** Computed separate slices along the longitudinal direction. Bar # 4
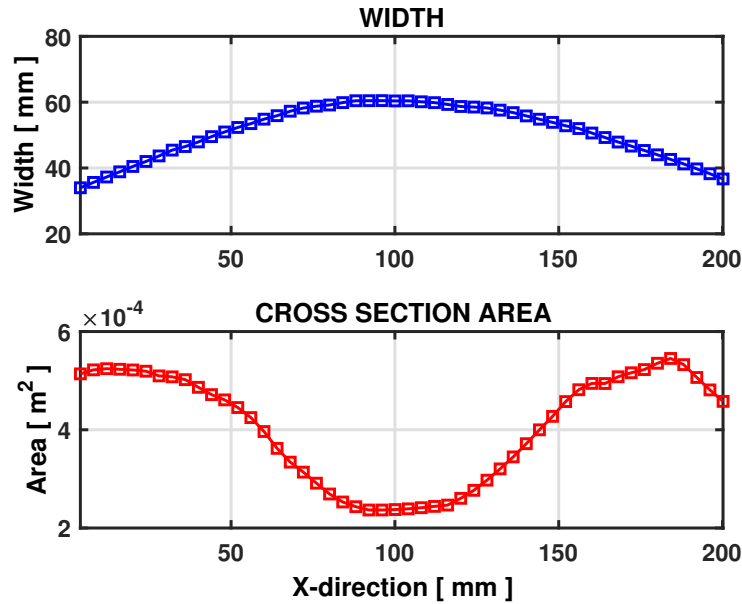
**Figure 6.3:** Estimated width and area along the longitudinal direction. Bar # 4

Modal computations were finally performed for the nine bars following the setup presented on Section 6.2. Figures 6.5-6.10 present the first six nonzero-frequency modes computed for bar # 4. As can be seen, the bar vibrates in the three directions, in different ways, including flexural, torsional and lateral motions, and the corresponding mode shapes are very similar to the vibrational modes found for marimba (Bork, I. et al., 1999; Beaton, D. and Scavone, G., 2019). Modes 1, 3 and 5 correspond to flexural modes, modes 2 and 4 to torsional modes while mode 6 combines both torsional and lateral motions. Notably, a quick comparison with the experimentally identified mode shapes displayed in Figures 4.9-4.13 show that the computed mode shapes are not only close to identical, but more detailed, since computations allow motions in every direction. Although not presented, the bar also presents six low-frequency modes that describe rigid-body motion, corresponding to translation and rotation of the bar, with near-zero frequencies.

It is then interesting to compare the modal frequencies computed and identified experimentally. Table 6.2 lists the frequency values stemming from the FE model for all the bars comprising the laboratory timbila. Also, Figures 6.11 plots the errors between predictions and measurements. In general, it shows that the modal frequencies are in general correctly estimated for the bending modes but differ largely for torsional modes. The mean relative error among the nine bars is less than 0.7% for the first bending mode and then increases with the frequency for the higher modes. They are about 4% and 12% for the second and third
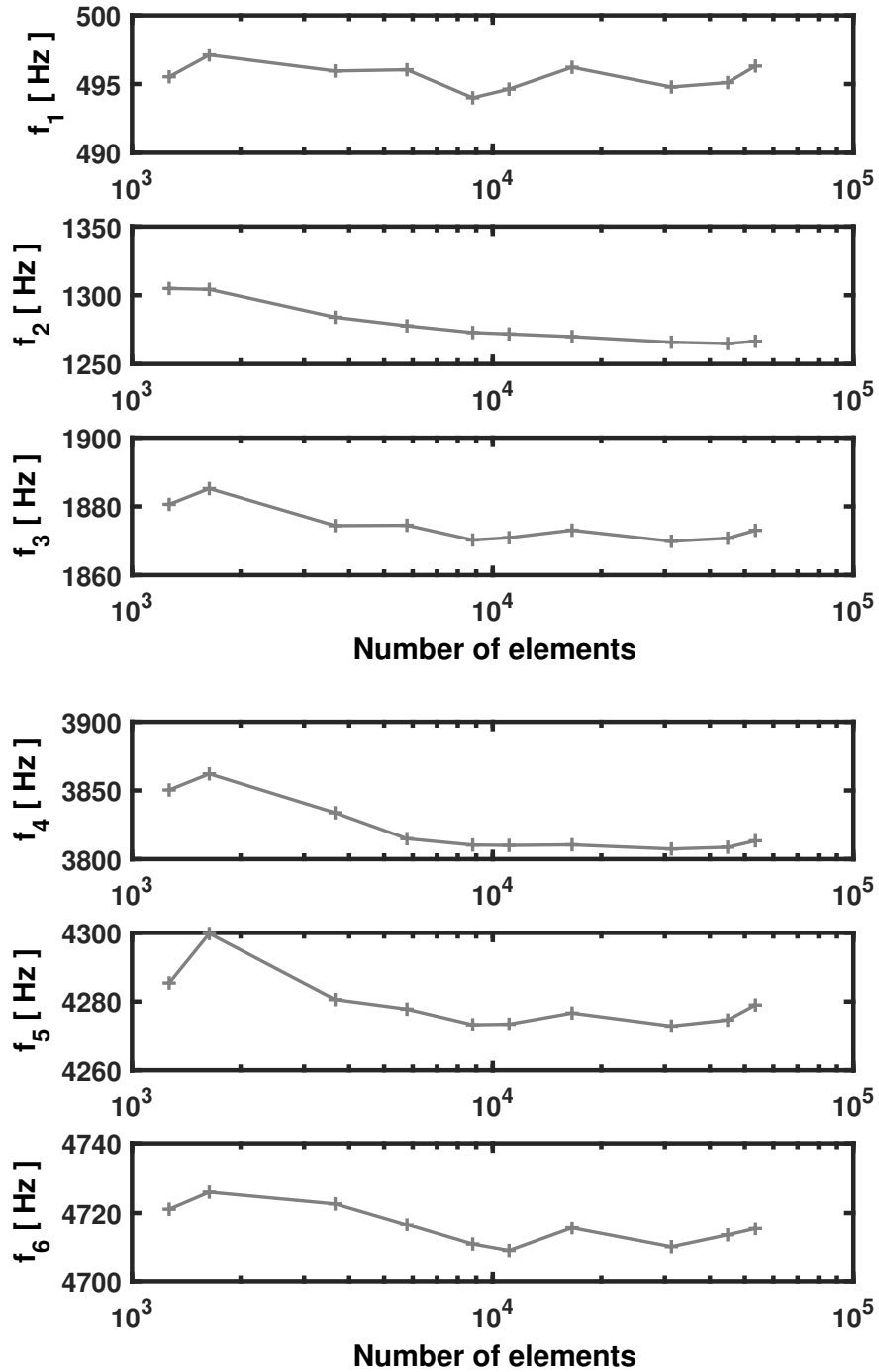
**Figure 6.4:** Convergence of modal frequencies for the first six computed modes.
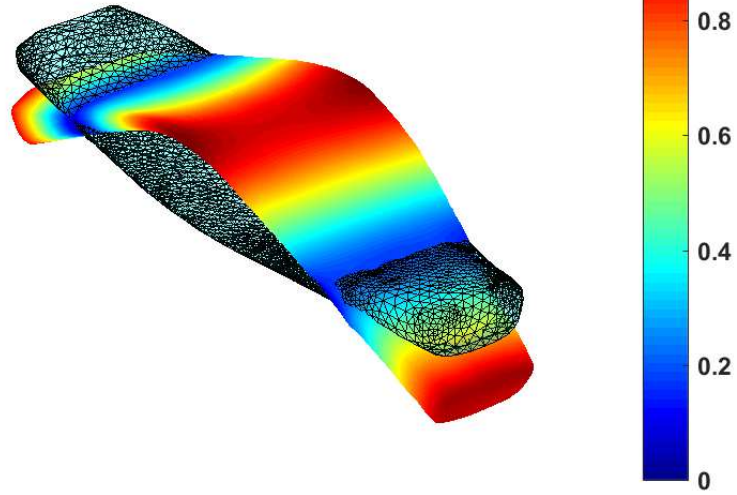
MODE 1 : 491.0 Hz



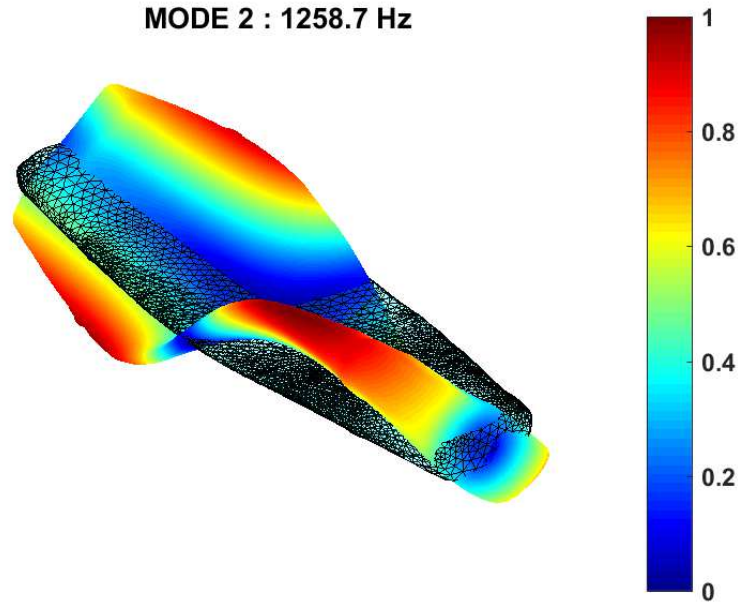**Figure 6.5:** First mode. Bar # 4.

MODE 2 : 1258.7 Hz


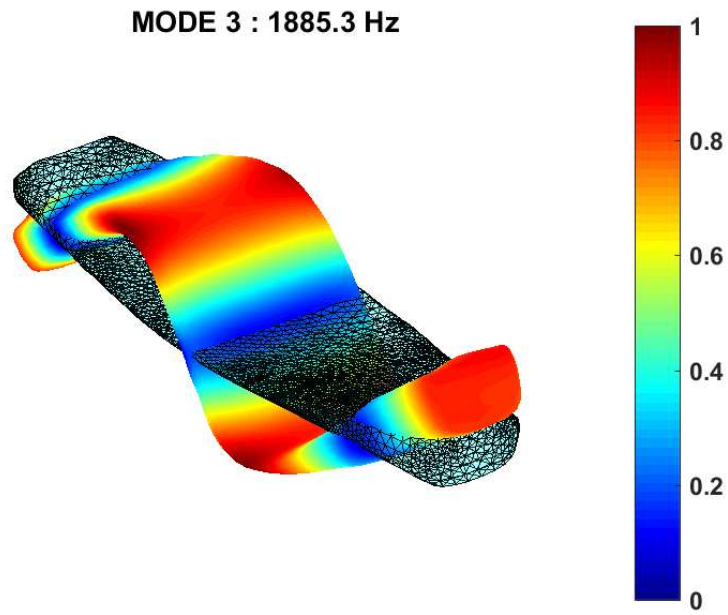
**Figure 6.6:** Second mode. Bar # 4.

**MODE 3 : 1885.3 Hz**



**Figure 6.7:** Third mode. Bar # 4.

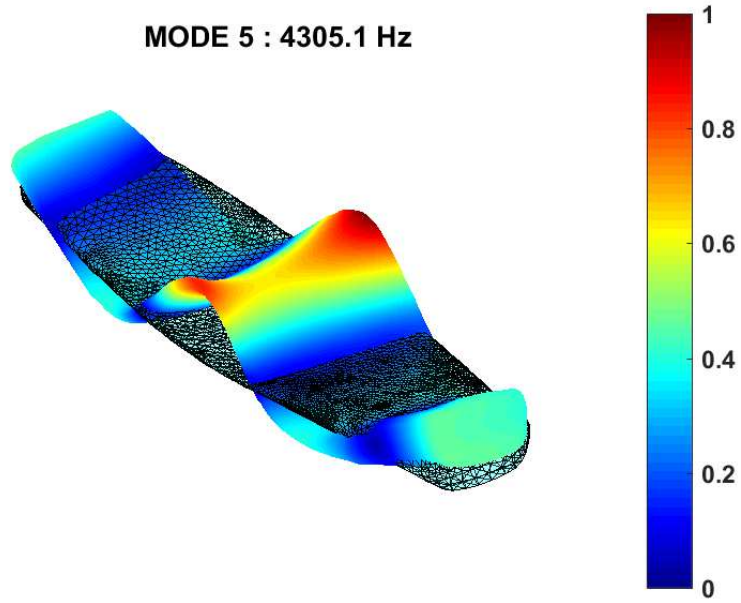**MODE 4 : 3821.4  Hz**
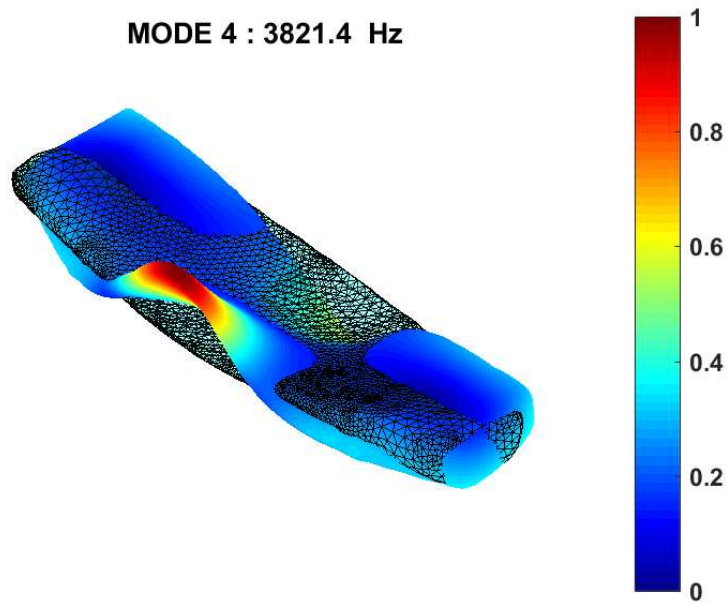


**Figure 6.8:** Fourth mode. Bar # 4.

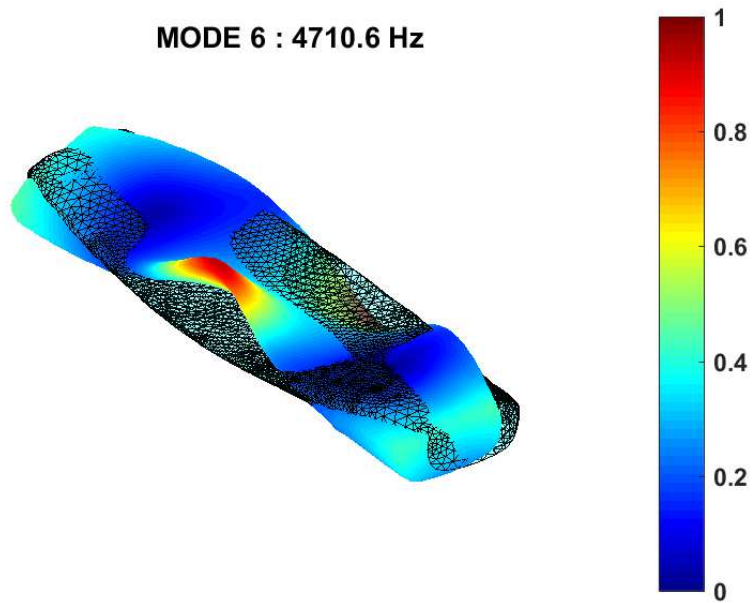**Figure 6.9:** Fifth mode. Bar # 4.



**Figure 6.10:** Sixth mode. Bar # 4.
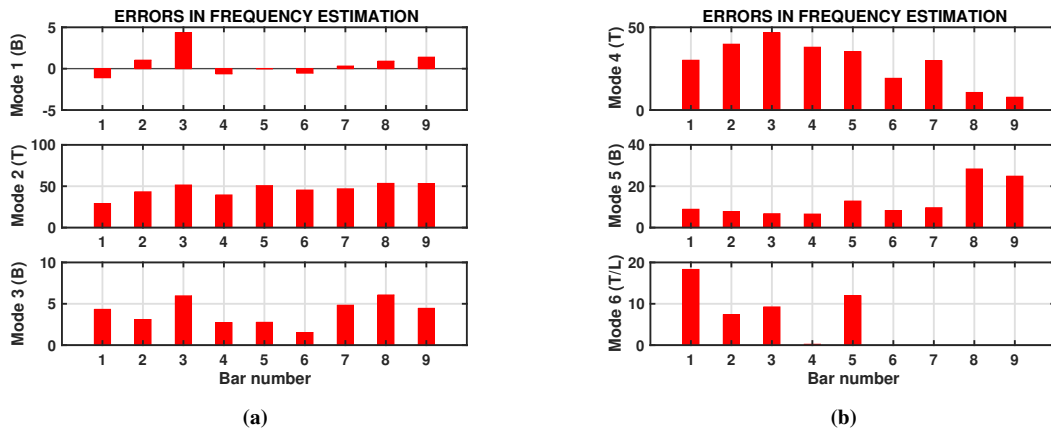
**Figure 6.11:** Error between FEM computed and experimentally identified modal frequencies.

modes respectively. As anticipated, the computed frequencies for modes involving torsional motions are not correctly predicted and always overestimated. This clearly shows the limits of performing modal computations using an isotropic FE model for bars.
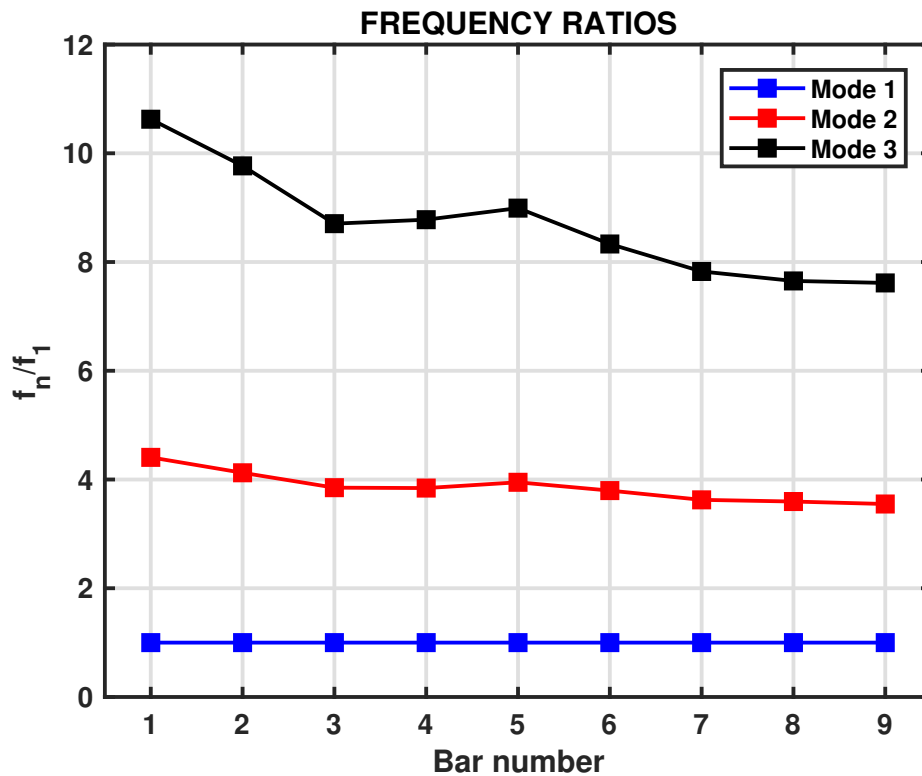


**Figure 6.12:** Internal frequency ratios between the first three bending modes of the laboratory timbila.

From the precise knowledge of the mode shape, it is then simple to analyze the tuning of the instrument. Since the sound produced is essentially due to vertical flexural waves, we focus our analysis on the frequency ratios between motion in this direction. As seen in Figure 6.12, this results in a series of natural frequencies with mean ratio of 1.00:3.84:8.77

for the first three bending modes, hence being far from integer ratios and in accordance with our results obtained by experimental modal analysis.

**Table 6.2:** FEM computed modal parameters of the laboratory timbila. Frequencies are presented in Hertz. B stands for bending modes, T for torsional modes and L for lateral modes.

| Bar number | 1 | 2 | 3 | 4 | 5 | 6 |
|---|---|---|---|---|---|---|
| 1 | 369.2 (B) | 958.5 (T) | 1627.1 (B) | 3262.8 (TL) | 3923.3 (B) | 4738.2 (T) |
| 2 | 412.6 (B) | 1093.8 (T) | 1701.4 (B) | 3611.5 (TL) | 4030.5 (B) | 4408.575 (T) |
| 3 | 463.3 (B) | 1174.0 (T) | 1783.6 (B) | 3629.4 (T) | 4033.3 (B) | 4487.9 (LT) |
| 4 | 491.0 (B) | 1258.7 (T) | 1885.3 (B) | 3821.4 (T) | 4305.1 (B) | 4710.6 (LT) |
| 5 | 546.7 (B) | 1424.1 (T) | 2158.8 (B) | 4188.6 (L) | 4915.6 (B) | 5143.5 (T) |
| 6 | 604.4 (B) | 1944.7 (T) | 2294.4 (B) | 4276.7 (L) | 5035.7 (B) | 5966.4 (T) |
| 7 | 670.3 (B) | 2098.8 (T) | 2430.4 (B) | 4450.8 (TL) | 5246. (B) | 6049.6 (T) |
| 8 | 745.9 (B) | 2459.8 (T) | 2681.4 (B) | 4225.6 (L) | 5707.7 (B) | 6920.0 (T) |
| 9 | 824.1 (B) | 2713.5 (T) | 2925.0 (B) | 4432.9 (L) | 6275.9 (B) | ∅ |

## 6.3 Accuracy in building 3D models from scan data

Before running modal computation for all the bars, we performed simple experiments to test the accuracy of the scanning process. As discussed in Section 5.1, capturing the bottom of the bars can be technically challenging, due to its difficult access for the scanner lights. This issue would be easily solved if one could dismantle the instrument, however, as our goal is developing a technique for historical instruments that cannot be disassembled, we decided to reproduce the working conditions we will face in real practical situation. The scanning of the laboratory timbila was done, therefore, with the bars attached to the structure.

To test our accuracy in scanning and our consistency in aligning scans and building 3D models, we perform one specific experiment consisting of comparing two 3D models of the same bar but obtained in different conditions. Since bar # 4 was loosely attached to the structure, we had the opportunity to perform a scan of the bar dissembled from the instrument, thus allowing easy access to the all bar geometry. The idea was to use the scan of the isolated bar as a reference and compare the resulting 3D model with a scan obtained from the same bar mounted on the instrument. As resumed in Table 6.1, we notice slight differences in the volume of the two models, less than 1%, which results in frequency difference of about 1% for the first three bending modes, which is a rather good agreement and shows that scanning is reliable, even for difficult-to-access parts of the instrument.

Further tests were performed to check the repeatability and reliability of the process

**Table 6.3:** Volume and FE-computed modal frequency differences between two 3D models of the same bar, mounted on and dismounted from the instrument.

|  | Disassembled | Assembled | Relative error |
|---|---|---|---|
| Volume (mm$^3$) | 83.28 | 82.46 | 0.8 % |
| $f_1$ (Hz) | 497.7 | 491.0 | 1.4 % |
| $f_2$ (Hz) | 1267.5 | 1258.7 | 0.7 % |
| $f_3$ (Hz) | 1878.6 | 1885.3 | -0.4 % |
| $f_4$ (Hz) | 3816.7 | 3821.4 | -0.1 % |
| $f_5$ (Hz) | 4292.4 | 4305.1 | -0.3 % |

of building 3D models. Indeed, errors in cleaning and aligning scans necessarily occur during the post-processing stage and results from our modal computations will strongly depend on the quality of the models. We therefore attempt to build several 3D models of the same bar by using as input the same raw scanned data and then compare them by looking at the geometry and at the computed modal frequencies obtained by FE modeling. To that end, attention was paid to build both the surface and solid models using a similar number of elements.

Table 6.3 shows the difference in the calculated volume and computed modal frequencies of the first bending modes for two models obtained from scratch. Not surprisingly, slight variations in the built geometry cause changes in the computed modal frequencies but notice that the relative errors between the modal frequencies remain less than 1%. During tests, it was noticed that the values of the modal frequencies were very sensitive to small changes in the thickness of the bar undercut, as known from xylophone instruments makers, so that excessive cleaning of the scans could lead to large errors in the modal frequencies (of about 5%).

**Table 6.4:** Volume and FE-computed modal frequency differences between two 3D models of the same bar.

|  | Model 1 | Model 2 | Relative error |
|---|---|---|---|
| Volume (mm$^3$) | 82.46 | 84.22 | -2.1 % |
| $f_1$ (Hz) | 491.0 | 496.0 | -1.0 % |
| $f_2$ (Hz) | 1258.7 | 1279.0 | -1.6 % |
| $f_3$ (Hz) | 1885.3 | 1871.4 | 0.7 % |
| $f_4$ (Hz) | 3821.4 | 3832.2 | -0.2 % |
| $f_5$ (Hz) | 4305.1 | 4332.5 | -0.6 % |

## 6.4   Physics-based sound synthesis

Physical modeling has become an increasingly active field of research in music acoustics. Contrary to abstract or signal-based synthesis which intends to generate sounds or model the sounds of musical instruments, the approach taken in physical modeling is to develop mathematical models of the physical phenomena involved in the sound production process. The idea is to derive a physics-based mathematical representation of the dynamical behavior of the components together with their coupling, and search for the actual solutions numerically by integrating the equations of motions over time. From the computed temporal responses, sounds can be finally obtained and parametric physically meaningful computations can be done to understand the influence of changes in the instrument design and/or in the control by the player.

The synthesis technique used in this work is called modal sound synthesis (Adrien, J.M., 1991) and follows the lines proposed by Henrique and Antunes (Henrique, L. and Antunes, J., 2003) for simulating percussion instruments. Starting from the knowledge of the modes of a bar computed by FE-modal computation, this approach provides to simulate the motion of the bar according to a given mallet excitation.

As illustrated in Figure 6.13, our physical model includes three ingredients:

(*a*) the multi-modal vibrational behavior of a free bar supported at two flexible fixtures, described mathematically by a set of ordinary differential equations;

(*b*) the motion of the mallet that impacts the bar with an initial velocity $v_0$;

(*c*) a nonlinear interaction force between the bar and the mallet related to the impact force given by the player.

### 6.4.1   Timbila bar dynamics

Although the dynamics of the bar also includes longitudinal and torsional motions, only the vertical motions of the bar, which are the most significant source of sound radiation, are considered here. For simplicity, we also assume that the wood material is homogeneous and isotropic. In view of the modal framework, the vertical motion of the bar $w(\mathbf{r}, t)$ at position
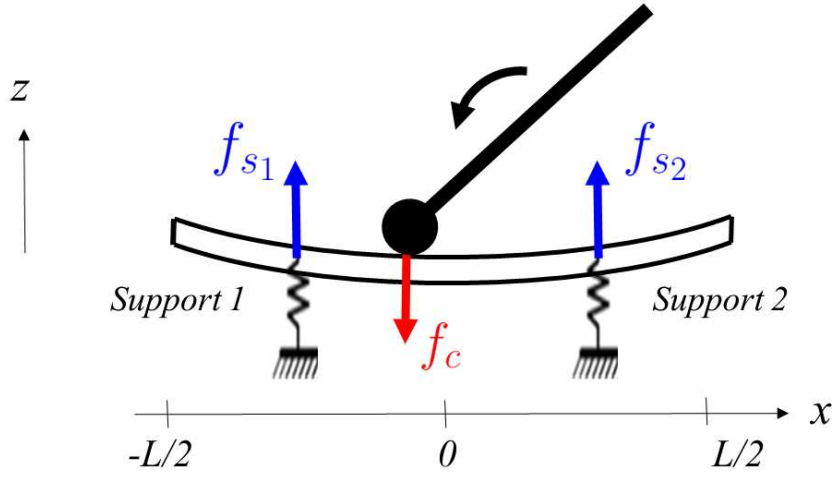
**Figure 6.13:** Description of the relevant quantities for physical modeling.

$\mathbf{r} = (x, y, z)$ and time $t$ is given by the sum of the modal responses,

$$w(\mathbf{r}, t) = \sum_{n=1}^{N} q_n(t)\varphi_n(\mathbf{r})$$  (6.2)

where $q_n(t)$ represents the contribution of each mode $\varphi_n(\mathbf{r})$, $\varphi_n(\mathbf{r})$ being the z-component of the 3D modeshape (along the vertical direction) and $N$ is the size of the modal basis. The time-dependent amplitudes of each mode is then governed by a set of $N$ second-order equations, written classically as:

$$m_n \ddot{q}_n(t) + c_n \dot{q}_n(t) + k_n q_n(t) = F_n(t)$$  (6.3)

where $m_n$, $c_n = 2m_n\zeta_n\omega_n$ and $k_n = m_n\omega_n^2$ are the modal masses, damping values and stiffnesses of the bar respectively, $\omega_n$ being the circular modal frequency and $\zeta_n$ the modal damping value which accounts for both internal material and acoustical dissipation. The term $F_n(t)$ represent the forces acting on each mode, which are obtained by projecting the physical force $f(\mathbf{r}, t)$ on the vertical component of every mode shape $\varphi_n(\mathbf{r})$ of the modal basis, as:

$$F_n(t) = \int_V f(\mathbf{r}, t)\varphi_n(\mathbf{r}) \, d\mathbf{r}$$  (6.4)

In this work, three localized forces acting in the direction perpendicular to the bar surface are considered to affect the dynamics of the bar:

(*a*) the mallet/bar interaction force related to the impact force $f_c(\mathbf{r}_c, t)$ of the player at

location $\mathbf{r}_c$ given by:

$$f_c(\mathbf{r}_c, t) = \mathsf{f}_c(t)\delta(\mathbf{r} - \mathbf{r}_c) \tag{6.5}$$

(*b*) the two support reactions at the attachment points of the cord on the bar $f_{s_1}(\mathbf{r}_{s_1}, t)$ and $f_{s_2}(\mathbf{r}_{s_2}, t)$ given by

$$f_{s_1}(\mathbf{r}_{s_1}, t) = \mathsf{f}_{s_1}(t)\delta(\mathbf{r} - \mathbf{r}_{s_1}) \tag{6.6a}$$

$$f_{s_2}(\mathbf{r}_{s_2}, t) = \mathsf{f}_{s_2}(t)\delta(\mathbf{r} - \mathbf{r}_{s_2}) \tag{6.6b}$$

Substituting Eqs. (6.5) and (6.6) in (6.4) and performing the integration on the bar geometry results in the following expression for the modal forces:

$$F_n(t) = \mathsf{f}_c(t)\varphi_n(\mathbf{r}_c) + \mathsf{f}_{s_1}(t)\varphi_n(\mathbf{r}_{s_1}) + \mathsf{f}_{s_2}(t)\varphi_n(\mathbf{r}_{s_2}) \tag{6.7}$$

where again $\varphi_n$ is the component of the 3D mode shape in the vertical direction.

## 6.4.2   Mallet dynamics

The mallet is then modeled as a rigid body of mass $m_z$, neglecting any elastic dynamics of the mallet beyond the contact deformation during the impact. Its normal motion is simply governed by Newton's law:

$$m_z \ddot{z}(t) = -f_w(\mathbf{r}_c, t) - m_z g \tag{6.8}$$

where $f_w(\mathbf{r}_c, t) \equiv f_c(\mathbf{r}_c, t)$ is the contact force that acts perpendicular to the bar upper surface at the mallet/bar contact point, $g$ is the gravitational acceleration and the minus sign comes from the convention that positive force acts toward positive vertical direction.

## 6.4.3   Mallet/bar interaction force

The bar/mallet interaction force $\mathsf{f}_c(t)$ must be now determined. To that end, a theoretical contact model between the bar and the mallet is needed. An elegant choice is given by the theory of linear elasticity developed by Hertz, referred to as the Hertz's law, for which the contact force, which acts perpendicular to the tangent plane including the contact point, is a

nonlinear power function of the local compression. The Hertz law expresses the interaction force $f_c(t)$ between two elastic contacting bodies as

$$\mathsf{f}_c(t) = K_c\,\delta(t)^b \tag{6.9}$$

where $\delta(t)$ is the relative normal deformation (compression) between the contacting solids, $b$ is typically equal to 3/2 for a sphere in contact with an elastic half-space and $K_c$ is a contact stiffness coefficient that depends on both surfaces geometries and the elastic properties of the two solids.

The simplicity of Eq.(6.9) makes Hertz's model particularly attractive for music acoustics applications. It allows to the control of the mallet's stiffness by means of the coefficient $K_c$ and the nonlinearity enables to reproduce the spectral changes observed in percussion sounds when the instrument is struck with different impact forces. The contact stiffness $K_c$ influences the contact time which controls the frequency spectra of both the excitation and the corresponding response. The harder the contact stiffness, the shorter the contact time and the wider the frequency range of the response. Also, for $b > 1$, the impact force increases with compression and high-frequency modes will be progressively increasingly excited, leading to sounds of brighter timbral qualities. Nevertheless, apart its compactness, Hertz's theory remains a crude representation of the real interaction dynamics. Strictly speaking, it cannot be readily applied to dynamical problems for which the contact force evolves with time, but a quasi-static approximation, as considered here, is a plausible pragmatic approach. The impact force is given by Hertz's law of contact:

$$\begin{cases} \mathsf{f}_c(t) & = & -K_c\big|z(t) - w(\mathbf{r}_c, t)\big|^b & \text{if} \quad z(t) < w(\mathbf{r}_c, t) \\ \mathsf{f}_c(t) & = & 0 & \text{if} \quad z(t) \geq w(\mathbf{r}_c, t) \end{cases} \tag{6.10}$$

where $z(t)$ and $w(\mathbf{r}_c, t)$ is the normal motion of the mallet and the bar respectively. In a modal description, when the mallet and the bar are in contact, Eq.(6.10) becomes

$$\mathsf{f}_c(t) = -K_c\big|z(t) - w(\mathbf{r}_c, t)\big|^b = -K_c\bigg|z(t) - \sum_{n=1}^{N} q_n(t)\varphi_n(\mathbf{r}_c)\bigg|^b \tag{6.11}$$

which highlights that all bar modes become coupled through the contact nonlinearity. This redistributes the impact energy across all the modes during the contact duration, even those

which were not excited initially.

### 6.4.4 Force at supports

On tuned keyboard percussion instruments, the "free-free" boundary conditions are obtained by attaching the bars together with a light and flexible cord, which act as flexible suspension and provide low-frequency rigid body modes (Chaigne, A. and Kergomard, J., 2016). Physically, the supporting fixture leads to reaction forces on the bar, which can be modeled as flexible-dissipative forces:

$$\mathsf{f}_{s_1}(t) = -K\,w(\mathbf{r}_{s_1}, t) - C\,\dot{w}(\mathbf{r}_{s_1}, t) \tag{6.12a}$$

$$\mathsf{f}_{s_2}(t) = -K\,w(\mathbf{r}_{s_2}, t) - C\,\dot{w}(\mathbf{r}_{s_2}, t) \tag{6.12b}$$

where $K$ and $C$ are arbitrary parameters describing the support stiffness and damping respectively. In practice, the value of the contact stiffness must be low in order to provide the coupling between the bar and structure without affecting the natural frequencies of the (tuned) bar.

### 6.4.5 Time-step integration

Equations (6.2), (6.3), (6.7), (6.8) and (6.10) represent the essential physics of the bar dynamics. It surely includes enough details to obtain satisfactory simulations obtained by time integration once initial conditions have been properly defined. There are many time-step integration algorithms which might compute the time-domain responses. In our implementation, we used the explicit velocity-Verlet integration scheme (Swope, W.C. et al., 1982) which is known to provide accurate results in the context of vibro-impacting systems. Basically, the dynamical quantities, i.e position, velocity and acceleration at time $t_{n+1} = t_n + \Delta t$ are computed from the corresponding quantities and the contact force at previous time $t_n$ using an adequate time step $\Delta t = 2\ 10^{-6}$ s. Here, the main difficulty comes from the short duration of the contact time which requires a small $\Delta t$ for stable and accurate computations.

## 6.4.6 Preliminary numerical results

The main objective is now to present illustrative results of our computational model with regard to what can be expected physically. In summary, the time-domain dynamical responses of the timbila bar to a mallet excitation are computed as follows:

1. Load the modal frequencies $f_n$, modeshapes $\varphi_n$ and modal masses $m_n$ computed by FE modal computations of a scanned bar;

2. Interpolate the bar modeshapes at the excitation $\varphi_n(\mathbf{r}_c)$ and supports locations $\mathbf{r}_{s_1}$ and $\mathbf{r}_{s_2}$;

3. Interpolate the modal damping values $\zeta_n$ for all the modes using values experimentally identified;

4. Define the initial impact velocity $v_0$, contact stiffness coefficient $K_c$, and simulation time;

5. Integrate the set of ($N$+1) modal equations in time;

6. Generate graphic outputs and sounds from the simulated bar responses.

Struck excitations were simulated by considering point-wise excitations, provided by a mallet of mass $m_z$=15 gr, with initial velocity $v_0$ and assuming a contact stiffness of $K_c = 10^8$ N/m$^{1.5}$ between the two solids. In order to ensure a weak coupling between the bar and the supporting fixture, we consider values for the support stiffness and dissipation of $10^4$ N/m and 10 Ns/m respectively, resulting in low frequencies for the flexible system made by the bar and the cord, at approximately 20 Hz and 40 Hz for the translation and rotation of the bar respectively.

Figures 6.14-6.15 show typical results obtained for one simulation of bar # 4, considering an impact velocity of $v_0 = 1$ m.s$^{-1}$, which is intended to reproduce fairly normal excitation by player. Figure 6.14 is a plot of the simulated excitation force. From the time representation, it can be seen that it has the expected symmetrical bell-shaped curve, with order of magnitude for the amplitude similar to measurements done on xylophone (Chaigne, A. and Doutaut, V., 1996). Also, the duration of the impact is very short, equal to 0.3 ms, which leads to a rich frequency content, as revealed by the frequency spectrum. Figure 6.15 then is a plot of the bar acceleration, in the form of a time-frequency analysis, obtained by short Fast Fourier Transform of overlapping segments of the simulated response data. After

the impact excitation that feeds vibrational energy into the modes of the bar, the bar starts vibrating in free response with a rapid decay. The analysis of the results in Figure 6.15 allows the frequencies to be extracted, with one strong component at 490 Hz, together with other five partials at the expected frequencies (see Table 6.2) that rapidly die away. Figure 6.16 then consists of comparing the bar response simulated at two different locations. As anticipated, the plots displayed in Figure 6.16 show similarities in their time response and frequencies contents. Their differences come from the mode shape values at the two locations, that lead to different modal recombination (see Equation (6.2) and different amplitudes for the frequency components. The main difference between the two signals is their out-of-phase motion that is evident from time 0.01 s and that can be explained by the fact that the bar rapidly vibrates according to its first mode, for which the center and extremities vibrate in opposite phase. Finally, Figure 6.17 illustrates the influence of the nonlinearity of the excitation. Variations of the impact velocity produce the expected changes in the force and responses signals. The case of weak and stronger excitation are considered by testing initial velocities of $0.1$ m.s$^{-1}$ and $1$ m.s$^{-1}$. As seen from Figure 6.17, a stronger excitation leads to a more energetic and shorter contact time and excites more efficiently a larger number of modes than a weak one, thus resulting in a brighter sound. On the contrary, using a weak excitation results in a gentle sound, favoring few low-order modes. Overall, these numerical experiments show that the presented model is able to reproduce and control the main features of both the bar and player's action. However, for a precise validation, these results have to be later extended by a series of tests, including a close comparison between real and simulated signals obtained in similar conditions, as well as perceptive listening tests.
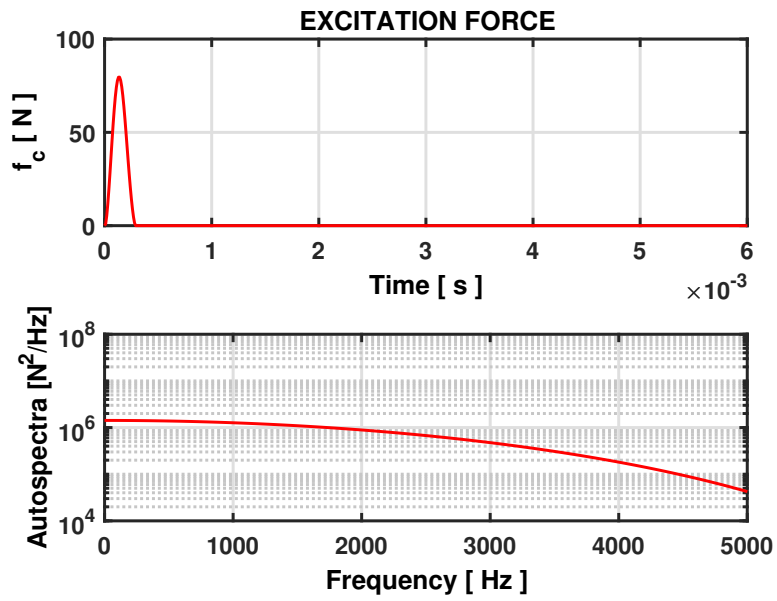
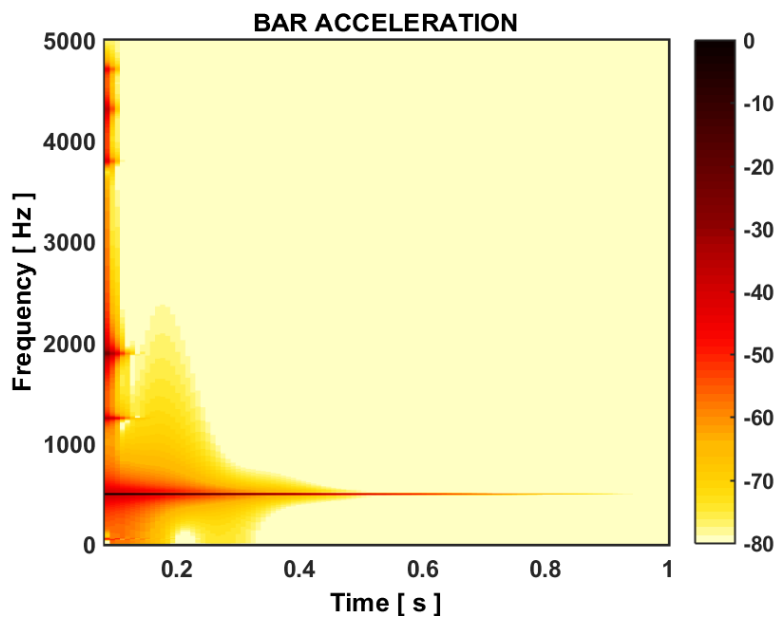**Figure 6.14:** Time history and autospectrum of the excitation force.



**Figure 6.15:** Spectrogram of the bar response close to the bar extremity. Bar # 4.
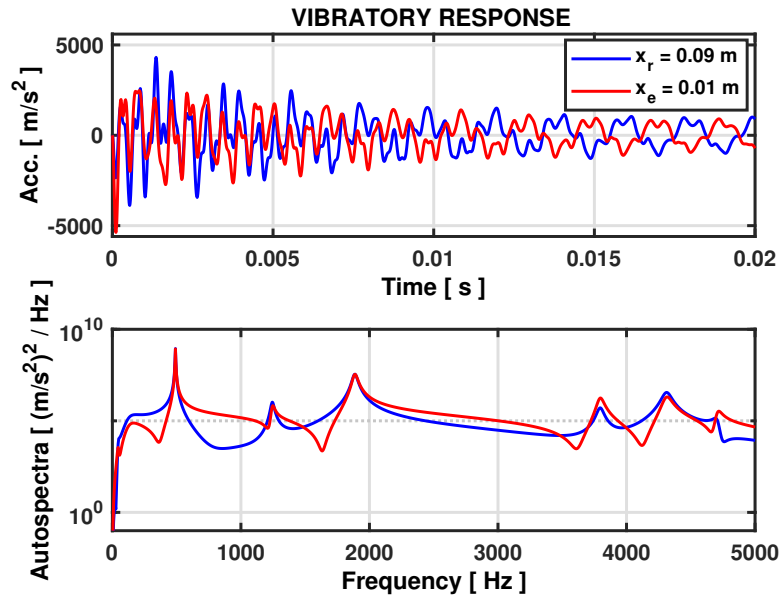
**Figure 6.16:** Time history and autospectrum of the bar response at two different locations. Bar # 4.
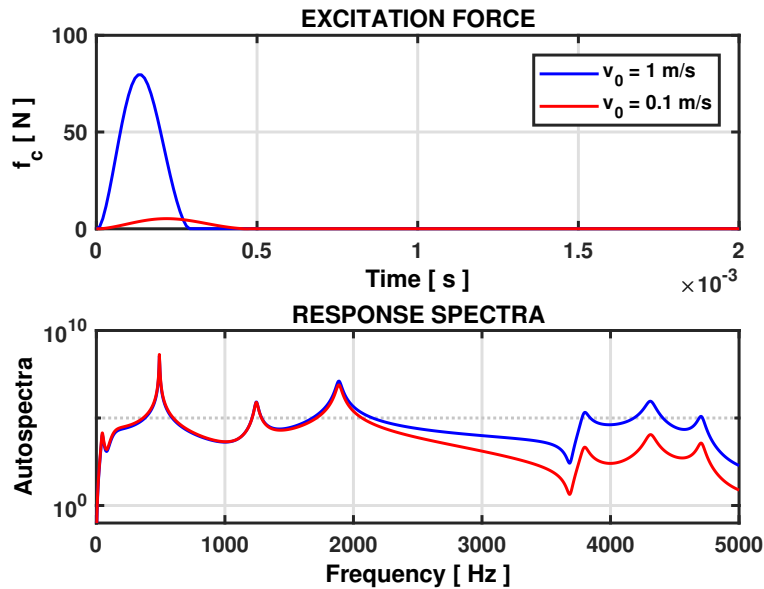


**Figure 6.17:** Time history of the excitation force and autospectra of the bar response for a weak (red) and a strong (blue) excitation. Spectra have been normalized to their energy contents for easy comparison. Bar # 4.

# Chapter 7

# Conclusion and perspectives

This dissertation devised a non-destructive strategy based on reverse engineering techniques aiming at assessing the musical features of timbila wooden xylophones. We explored the full potential of the 3D scan technology to obtain 3D models of bars of real instruments, and process the acquired data for extracting important geometrical features and for computing their relevant vibrational properties through Finite Element modal analysis. From the knowledge of these data, we also developed a modal sound synthesis technique based on physical approach, that simulates the transient response of timbila bars to a struck excitation and provides realistic synthetic sounds. The proposed techniques were compared with experimental data from a real instrument and a systematic workflow was proposed to be later performed efficiently on historical timbilas housed by the National Museum of Ethnology of Lisbon.

The proposed methodology takes advantages of the scanning technology, which is by nature contacless, and proves to be a powerful tool for modeling and analysis purposes of musical instruments. We succeeded in creating a faithful digital version of the wooden bars that allows to analyze their geometry in details, including the bar undercut whose shape is fundamental for tuning. Besides such applications, this digital recreation could be also used towards other goals, including the construction of instrument replicas by 3D printer or the development of interactive applications for virtual museology.

As for the modal computation results, the method proved to be accurate on

predicting the modal frequencies of the bending modes, which are the most important for sound radiation. The prediction of the torsional modes however were far from being accurate using the simplified isotropic model for wood material. Nevertheless, the fundamental mode is surely the most important, especially for pitch perception, and seems the only modes tuned by timbila makers. However, for faithfully reproducing timbral qualities, it is surely important to correctly predict all the bar overtones.

For achieving the desired model, there are a few steps to be accomplished, which will be developed on the continuation of this project. The first one is to develop an orthotropic FEM model for timbila bar so that the characterization of the wood mechanical properties is essential for future work. Having the detailed characterization of the wood properties along the three axis, we will be finally able to predict both bending and torsional low-frequency modes reasonably. We already perform numerical experiment with an orthotropic model for the bar on our FEM module, using as inputs the mechanical properties of a similar wood and results are encouraging. This shows that, once we will have the knowledge of the Mwenje mechanical properties on three axes, it may be possible to predict many modes correctly.

Assessing the mechanical properties of the *Mwenje* through vibratory tests will not only allow us to analyze the sound of timbilas, but will also serve as a guide to find sustainable alternatives to the use of this wood in the construction of modern timbilas. Considering the *Mwenje* comes from a tree in the process of extinction, UNESCO pointed the preservation of this tree as one of the most urgent actions to the safeguarding of the timbila.

Other issue to be rigorously addressed over the next future will be the bar/membrane/resonator interaction, to best reproduce the sonic subtleties of the timbila. So far, we have only synthesized the sound of an isolated bar excited by a mallet, with no resonator interacting. In order to faithfully reproduce the functioning of the timbila, we need to add to it the effect of the resonators and the membrane.

For the future work on the museum, experimental modal analysis using contactless laser measurement will be also necessary. One reason is that the knowledge of modal damping, which is associated with sound decay, can only be made in a simple way from modal tests. Another reason is that having the experimentally identified mode frequencies is crucial to be used as parameter to compare with FEM computed results, in order to confirm

the accuracy of the scanning and the adjustment FEM model.

In summary, the workflow to be followed on the museum will be:

1. Modal identification with hammer+laser measurements;

2. 3D scanning of the bars;

3. FEM modeling and modal computation of bars;

4. 3D scanning of the resonators;

5. Couple mallet, bar, resonator and membrane effects to perform sound synthesis by physical modeling.

By applying this method on the timbilas of the National Museum of Ethnology , we will be able to virtually resurrect the world's largest timbila collection. This collection has been held in the museum storage for more than 50 years, without ever being exposed to the public. With this project, we hope to finally give it the deserved attention, making justice to these historical instruments and the musical tradition they represent.

# Bibliography

Adrien, J.M. The missing link: Modal synthesis. In G. DePoli, A. Picalli, and C. Roads, editors, *Representations of musical sounds*. MIT Press, Cambridge, 1991.

Agencia Lusa. Governo de moçambique vai defender chope timbila, património da humanidade, 2020. URL https://www.rtp.pt/noticias/cultura/governo-de-mocambique-vai-defender-chope-timbila-patrimonio-da-humanidade_n155561.

Aramaki, M., Baillères, H., Brancheriau, L., Kronland-Martinet, R., and Ystad, S. Sound quality assessment of wood for xylophone bars. *The Journal of the Acoustical Society of America*, 121:2407–2420, 2007.

Beaton, D. and Scavone, G. Measurement-based comparison of marimba bar modal behaviour. In *Proceedings of the International Symposium in Music Acoustics*, 2019.

Bork, I., Chaigne, A., Trebuchet, L.-C., Kosfelder, M., and Pillot, D. Comparison between modal analysis and finite element modelling of a marimba bar. *Acustica-Acta Acustica*, 85:258–266, 1999.

Campbell, M. and Kenny, J. Acoustical and musical properties of the deskford carnyx reconstruction. In *Proceeding of Acoustics 2012 Nantes*, 2012.

Carvalho, J. S. de. Makwayela: choral performance and nation building in mozambique. *Horizontes Antropológicos*, 5:145–182, 1999.

Chaigne, A. and Doutaut, V. Numerical simulations of xylophones: I time-domain modeling of the vibrating bars. *Journal of the Acoustical Society of America*, 101:539–557, 1996.

Chaigne, A. and Kergomard, J. *Acoustics of musical instruments*. Springer, 2016.

Conte, S. L., Moyne, S. L., Ollivier, F., and Vaiedelich, S. Using mechanical modelling and experimentation for the conservation of musical instruments. *Journal of Cultural Heritage*, 13:145–182, 1999.

Cuadra, de la, P., Vergez, C., and Causse, R. Use of physical-model synthesis for developing experimental techniques in ethnomusicology-the case of the oudeme flute. In *Proceedings of the ICMC conference 2002*, 2002.

de La Caille, N.L. *Journal historique du voyage fait au Cap de Bonne-Espérance: précédé d'un Discours sur la Vie de l'Auteur, siuvi de remarques & de réflexions sur les Coutumes des Hottentots & des Habitans du Cap*. Guillyn, 1763.

de Weck, O. Y. and Kim, I. Y. *Finite Element Method. Engineering Design and Rapid Prototyping*. Massachusetts Institute of Technology, 2004.

Debut, V., Kergomard, J., and Laloe, F. Analysis and optimisation of the tuning of the twelfths for a clarinet resonator. *Applied Acoustics*, 66:365–409, 2005.

Debut, V., Carvalho, M., and Antunes, J. Objective estimation of the tuning features of historical carillons. *Applied Acoustics*, 101:78–90, 2016a.

Debut, V., Carvalho, M., Figueiredo, E., Antunes, J., and Silva, R. The sound of bronze: Virtual resurrection of a broken medieval bell. *Journal of Cultural Heritage*, 19:544–554, 2016b.

Dias, M. Instrumentos musicais de mooçambique. *Geographica, Revista da Sociedad de Geografia De Lisboa*, 6:2–17, 1966.

Dos Santos, J. *Ethiopia oriental e varia historia de cousas notaveis do oriente*. mpressa no Convento de S. Domingos de Euora por Manoel de Lira impressor, 1609.

Fletcher, N. H. and Rossing, T. D. *The physics of musical instruments*. Springer Science & Business Media, New York, 1998.

Fu, Z.F. and He, J. *Modal Analysis*. Elsevier Science, 2001.

Green, D. W., Winandy, J. E., and Kretschmann, D. E. *Mechanical properties of wood. Wood handbook : wood as an engineering material*, chapter 4. USDA Forest Service, Forest Products Laboratory, Madison, WI, 1999.

Henrique, L. *Concepção e caracterização de instrumentos musicais de lâminas utilizando técnicas de modelação e optimização*. PhD thesis, NOVA/FCSH, 2004.

Henrique, L. and Antunes, J. Optimal designs and physical modeling of mallet percussion instruments. *ACTA Acustica*, 89:948–963, 2003.

Jones, A. M. *Africa and Indonesia: the Evidence of the Xylophone and Other Musical and Cultural Factors*. Leiden: E. J. Brill, 1964.

Juang, J. *Applied System Identification*. PTR Prentice-Hall, Inc., New Jersey, 1994.

Junod, H. A. The mbila or native piano of the tshopi tribe. *Bantu Studies*, 3:275–285, 1929.

Kirby, P. R. *Musical instruments of the indigenous people of South Africa*. Johannesburg: Witwatersrand University Press, 2013.

Linz, P. and Wang, R. *Exploring Numerical Methods: An Introduction to Scientific Computing Using MATLAB*. Jones and Bartlett Publishers, 2003.

Lutero, M. and Pereira, C. M. A música tradicional em moçambique. *Africa*, 2:575–588, 1980.

Plant Ressources. Plant ressources of tropical africa, 2020. URL `https://www.prota4u.org/database/protav8.asp?g=psk&p=Ptaeroxylon\%20obliquum`.

Swope, W.C., Andersen, H.C., Berens, P.H., and Wilson, K.R. A computer simulation method for the calculation of equilibrium constants for the formulation of physical clusters of molecules: application to small water clusters'. *Journal of Chemical Physic*, 76:637–649, 1982.

Szilvasi-Nagy, M. and Matyasi, G. Analysis of STL file. *Mathematical and computer modelling*, 38:945–960, 2003.

Tabatabaian, M. *Comsol for engineers*. Comsol for engineers, 2014.

Theal, G. M. C. *Records of South-Eastern Africa: collected in various libraries and archive departments in Europe*. Government of the Cape Colony, 1898.

Tracey, A. Chopi timbila music. *African Music: Journal of the International Library of African Music*, 9(1):[7]–32, Nov. 2011.

Tracey, H. *Chopi Musicians. Their music, poetry, and instruments*. Oxford University Press, 1948.

Tracey, H. Musical wood. *African Music Society*, 1:17–21, 1949.

UNESCO. Convention for Safeguarding of the Intangible Cultural Heritage. Paris, 2003.

Wane, M. A timbila chopi: Construção de identidade étnica e política da diversidade cultural em moçambique (1934-2005). Master's thesis, Universidade Federal da Bahia, Brazil, 2010.

Wangemann, D. *Ein zweites Reisejahr in Süd-Afrika*. Berlin, 1898.

Warneke, N. Non destructive and multidisciplinary methods for the identification of african xylophones in portuguese collection. Technical report, COST Action WOOD MUSICK, July 2014.

Zhang, C. and Tsuhan, C. Efficient feature extraction for 2d/3d objects in mesh representation. In *Proceedings 2001 International Conference on Image Processing*, volume 3, pages 935–938, 2001.